Journal of Pharmacology and Drug Delivery

ScitechJournals

Open Access

Photoremovals of Vancomycin, Doxycycline and Clindamycin Antibiotics via Graphene Oxide Decorated with Copper Oxide (GO-CuO) Nanocomposites under Sun Light

Abstract

Pharmaceutical contaminants have become a major source of pollution in water resources worldwide, with growing awareness of their profound health and environmental consequences. Therefore, the development of efficient, cost-effective, and sustainable methods for removing or degrading these pollutants from water is essential. Herein, the raphene oxide nanosheets decorated with copper oxider (GO-CuO) nanocomposite was prepared for the effective photocatalytic degradation of Vancomycin, Doxycycline and Clindamycin antibiotics in water. The structural and morphological properties of the prepared GO-CuO nanocomposite were thoroughly investigated using XRD, SEM, EDX, and AFM analyses. These studies showed that the as-prepared nanocomposite has a crystalline structure having the average size of 25 nm with high elemental purity and rough morphology. The synthesized GO-CuO nanocomposite photocatalyst was further employed for the degradation of Vancomycin, Doxycycline and Clindamycin antibiotics. By optimizing key experimental parameters, such as catalyst dosage (1 mg/L), proton source (NaBH4) and its optimum concentration (0.002 M), and sunlight exposure duration (7 min), an exceptional 99.00%, 98.70% and 98.90% maximum photodegradation yields of Vancomycin, Doxycycline and Clindamycin antibiotics were achieved respectively. For the aforementioned high yields the sun ligth power, nanocomposite concentration, Vancomycin, Doxycycline and Clindamycin concentrations, pH and temperature should be 40 W/m2, 1 mg/L, 3000 mg/L, 7.0 and 30oC, respectively. This remarkable outcome highlights the excellent photocatalytic performance of the GO-CuO nanocomposite. Moreover, the as-prepared GO-CuO-based photocatalyst can be effective at large-scale for the degradation of other antibiotics after optimization. The photodegradation reaction kinetic of Vancomycin, Doxycycline and Clindamycin antibiotics followed the pseudo second-order Lagergren model with high R2 valus and kinetic rate constants. After the 6th cycle, the degradation performance of GO-CuO nanocomposite for Vancomycin, Doxycycline and Clindamycin antibiotics were observed as 88.40-89.21%, which is good for a heterogeneous catalyst.

Research Article

Delia Teresa Sponza[1], Rukiye Oztekin[1]*

[1]Department of Environmental Engineering, Dokuz Eylül University, Tınaztepe Campus, 35160 Buca/ Izmir, Turkey

***Correspondence:** Rukiye Oztekin, Department of Environmental Engineering, Dokuz Eylül University, Tınaztepe Campus, 35160 Buca/Izmir, Turkey, E-mail: rukiyeoztekin@gmail.com

Received: 06 July 2026; **Accepted :** 20 July 2026; **Published :** 28 July 2026

Keywords: Clindamycin; Doxycycline; Graphene oxide decorated with copper oxide (GO-CuO) nanocomposites; Pharmaceutical contaminants; Photoremoval; Sunlight; Vancomycin.

Introduction

Water is an essential element for sustaining life [1]. Over the past few decades, its usage has grown significantly across domestic, agricultural, and industrial sectors, resulting in a decline in water quality. The variety and harmful nature of pollutants released by different industries pose a serious challenge [2-5]. In recent years, growing attention has been directed toward emerging contaminants such as pharmaceutical compounds (PCs) due to their harmful effects on the ecosystem [6-10]. The effluents produced by pharmaceutical manufacturing industries often end up in domestic wastewater systems, natural water bodies such as rivers, lakes, and ponds, as well as in soils, sediments, and plants [11-15]. However, the recent studies have shown that the effluents released from pharmaceutical industr have shown that the effluents released from phar-

maceutical industries in all countries contain significantly higher levels of antibiotic drugs compared to other regions of the world [16]. Among pharmaceutical compounds, antibiotic drugs have received the most attention due to their role in the development of Antibiotic-Resistant Bacteria (ARB) and Antibiotic-Resistant Genes (ARGs). However, the presence of ARB and ARGs in water bodies not only disrupts aquatic ecosystems but also poses significant risks to human health as well as [17,18].

Vancomycin (C66H75Cl2N9O24) is a powerful glycopeptide antibiotic used primarily to treat serious, life-threatening bacterial infections caused by Gram-positive bacteria [19-25]. It is often considered a “drug of last resort” when other antibiotics fail or when infections are resistant to standard treatments. It is a natural branched, tricyclic, glycosylated non-ribosomal peptide produced by the soil bacterium Amycolatopsis orientalis. Molecular Formula: Here is a comprehensive summary of technical and medical information about Vancomycin: It is the gold standard treatment for Methicillin-resistant Staphylococcus aureus (MRSA). Used for endocarditis (heart valve infection), osteomyelitis (bone infection), sepsis, and lower respiratory tract infections. Taken orally to treat severe intestinal inflammation (Clostridioides difficile-associated diarrhea). Vancomycin must be given through an IV for systemic infections. It is a large, hydrophilic molecule that cannot be absorbed into the bloodstream from the gut. Given orally only to treat localized gut infections like C. difficile colitis. It works directly inside the intestines and does not treat infections in other parts of the body when swallowed. Vancomycin works by inhibiting the synthesis of the bacterial cell wall. It binds tightly to the D-alanyl-D-alanine terminus of cell wall precursor units, preventing the bacteria from building its protective outer layer and causing it to burst (lysis). An infusion-related reaction characterized by intense flushing, rash, or redness on the face, neck, and upper body. It is caused by rapid IV administration triggering histamine release can cause kidney damage, especially when used in high doses or combined with other kidney-toxic drugs. May cause damage to hearing or balance organs, leading to tinnitus or hearing loss. Nausea, stomach pain, and low potassium levels [19-25].

Doxycycline (C22H24N2O8) is a broad-spectrum tetracycline antibiotic used to treat a wide variety of bacterial infections and certain parasite-related conditions [26-29]. It works by stopping bacteria from making proteins essential for their growth, preventing them from multiplying. According to health authorities like Harvard Health and Medline Plus, this medication is commonly prescribed for: It treats acne vulgaris and rosacea by killing pore-infecting bacteria and reducing inflammation. It is used for pneumonia, bacterial bronchitis, and sinusitis. It is the primary treatment for Lyme disease, Rocky Mountain spotted fever, and infections spread by lice or mites. It treats infections such as chlamydia, gonorrhea, and syphilis. It is taken prophylactically by travelers visiting malaria-prone regions. Swallow the pill with a full glass of water and sit or stand upright for at least 30 min afterward to prevent severe throat and stomach irritation. Avoid taking it with dairy products (milk, yogurt), calcium, iron, zinc, or antacids. These bind to the antibiotic and stop your body from absorbing it. Take these items 2 h before or 1 h after your dose. Always finish the entire prescribed course, even if symptoms disappear, to avoid antibiotic resistance. Key Risks and Side Effects Medical insights from the U.S. FDA list important side effects and precautions: It makes your skin highly sensitive to sunlight, causing you to sunburn very easily. It is generally not approved for children under 8 years old because it can cause permanent tooth discoloration and affect bone development. It should be avoided by pregnant or breastfeeding individuals due to potential risks to the developing fetus or infant. Nausea, vomiting, diarrhea, and a higher risk of developing vaginal yeast infections during prolonged use. This antibiotic is ineffective against viral infections such as colds or the flu [26-29].

Clindamycin (C18H33ClN2O5S) is a lincosamide antibiotic used to treat serious bacterial infections [30-33]. It works by inhibiting bacterial protein synthesis, effectively slowing or stopping the growth of bacteria. Clindamycin is Lincosamide antibiotic. Binds to the 50S ribosomal subunit of bacteria to block protein synthesis. Primarily bacteriostatic (stops bacteria from reproducing), but can be bactericidal (kills bacteria) at higher concentrations against certain organisms. Effective against severe acne, soft tissue infections, and cellulitis. Frequently used to treat osteomyelitis. Used to treat Pelvic Inflammatory Disease (PID) and other internal infections, often combined with other medications. Prescribed for serious conditions like pneumonia or abscesses in the lungs. Serves as a primary alternative for patients allergic to penicillin, particularly for dental or strep infections. Available as capsules (e.g., brand name Dalacin C or Cleocin) and oral solution. Administered via Intravenous (IV) or Intramuscular (IM) injection in hospital settings. Formulated as gels, lotions, or solutions for acne and vaginal infections. Diarrhea, nausea, vomiting, abdominal pain, and skin rashes. Clindamycin can alter normal colon flora, leading to an overgrowth of Clostridioides difficile (C. diff). This can cause severe, life-threatening pseudomembranous colitis (severe inflammation of the colon). Should not be used by individuals with a history of hypersensitivity to lincosamides, or those with specific inflammatory bowel conditions. Clindamycin is a strong antibiotic medicine used to treat serious bacterial infections. It works by stopping bacteria from growing and multiplying. Doctors prescribe it when other antibiotics like penicillin

do not work. Here are important facts about clindamycin: It treats skin, bone, joint, and lung infections. It is also used for severe throat and dental infections. It belongs to a group of medicines called lincosamides. It stops bacteria from making the proteins they need to survive. You can take it as a capsule, apply it as a gel or cream, or get it through an injection in a hospital [30-33].

Up to date, different methods have been investigated for the removal of the Vancomycin, Doxycycline and Clindamycin antibiotics drug residues from wastewater systems, such as membrane filtration, advanced oxidation processes, chemical oxidation coagulation/flocculation, the fenton process, and adsorption [19-25]. However, each method has its own drawbacks, such as low efficiency, high costs, and time-consuming protocols. Nevertheless, the established techniques exhibit various notable limitations including time inefficiency, ineffectiveness, and high cost, rendering them unsuitable for commercial application. Among conventional approaches, photocatalytic oxidation is an energy-efficient and highly effective method for eliminating water contaminants such as antibiotic drugs and other organic impurities from the aqueous system. This approach decomposes pollutants by converting them into less hazardous substances like water and carbon dioxide, thereby preventing the formation of secondary pollutants. A widely used water treatment method utilizes heterogeneous photocatalysts, which promote oxidation and reduction processes involving organic compounds, hydroxyl ions, or oxygen molecules [34-43]. Moreover, the key advantage of photocatalysis over adsorption lies in its ability to completely mineralize pollutants rather than simply transferring them to a different phase; while adsorption concentrates pollutants onto a surface requiring subsequent disposal or regeneration, photocatalysis uses light-activated catalysts to generate reactive species that break down organic contaminants into harmless byproducts like CO2 and water, providing a more sustainable and thorough remediation process [44-50]. In recent decades, GO has been the subject of extensive research due to its exceptional properties, including a high surface area, excellent electron mobility, good transmittance, and unique optical, mechanical, and electronic characteristics, along with various other chemical and physical attributes [30-33]. In addition, these unique characteristics set GO apart from other nanomaterials, sparking considerable scientific interest and exploration [51-54]. The unique properties of GO have rendered it an incredibly versatile material, with diverse applications in state-of-the-art fields such as fuel cells, solar energy, gas sensors, supercapacitors, spintronics, biomedical technologies, separation processes, electrocatalysis, and photocatalysis, among others [26-29]. Further, In order to improve its electrical and thermal properties, GO has been surface-modified using a range of functionalizing agents, including polymers, biomolecules, inorganic nanoparticles, and organic compounds [55-58]. Metal oxide nanoparticles have garnered significant interest as surface functionalizing agents because of their capability to improve electrical, mechanical, and photoelectric properties and provide a high surface area [59,60]. CuO is a naturally generated p-type semiconductor with an indirect theoretical band gap of around 1 eV and an empirically observed band gap of roughly 1.2 eV [61]. CuO is widely employed in many different sectors because of its unique chemical and physical characteristics, such as a large specific surface area and substantial absorption of solar radiation [62]. These characteristics motivated us to develop nanocomposites by applying premium CuO nanoparticles on GO surfaces in an economical manner. Several possible environmental applications are made possible by graphene-based nanocomposites' capacity to absorb visible light. In order to detoxify wastewater polluted by different industrial effluents, we concentrated on creating extremely effective catalysts, building on earlier work in the environmentally benign production of metal oxide nanoparticles. CuO/GO nanocomposites were thus prepared, and they turned out to be excellent for environmental catalytic uses.

In this work, GO-CuO nanocomposite-based photocatalyst was synthesized for the photodegradation of Vancomycin, Doxycycline and Clindamycin antibiotics in water. The structural and morphological properties of the GO-CuO nanocomposite were investigated using XRD, SEM, EDX, and AFM analyses. The effects of GO-CuO nanocomposite dosages (0.2 mg/L, 0.5 mg/L, 1 mg/L, 2 mg/L and 3 mg/L) , proton concentrations (0.001 M, 0.002 M, 0.003 M and 0.004 M)), sunlight exposure duration (2 min, 5 min, 7 min, 9 min and 12 min), sun ligth powers (20 W/m2, 40 W/m2, 50 W/m2 and 60 W/m2), antibiotic concentrations (300 mg/L, 500 mg/L, 1000 mg/L, 2000 mg/L, 3000 mg/L and 4000 mg/L Vancomycin, Doxycycline and Clindamycin concentrations, separately), pH values (4.0, 7.0, 8.0 and 11.0) and temperatures (20°C, 30°C, 40°C and 50°C), on the photoremoval yields of Vancomycin, Doxycycline and Clindamycin antibiotics were investigated,respectively. Furthermore, the reusability of GO-CuO nanocomposite and photo degradation kinetics of aforementioned antibiotics were also investigated.

Materials and Methods

Synthesis of graphene oxide nanosheets

A modified Hummer's method was used to synthesize GO [30]. The precursor was high-purity graphite powder (99.99%). One hundred milliliters of sulfuric acid (H2SO4) and two grams of graphite powder were combined in an ice bath. Following that, 8 g of potassium permanganate (KMnO4) was added gradually while being constantly

stirred, and the reaction was left to continue for two hours. The final solution was diluted with 100 mL of deionized (DI) water, stirred for an hour, and then 20 mL of 30% hydrogen peroxide (H2O2) was added to reduce KMnO4, which caused a large release of bubbles and changed the color of the mixture from black to bright yellow. The suspension was subsequently rinsed three times with 5% hydrochloric acid (HCl) and then centrifuged for 20 min at 6000 rpm to achieve a pH of neutral. The purified GO solution was followed by filtering and dried at 60°C.

synthesis of GO-CuO nanocomposite material

A solution of 1.5 mg/mL GO was dissolved in 50 mL of deionized (DI) water and ultrasonically agitated for two hours at room temperature. Then, CuCl2 was added to the GO suspension with a same ratio of (1:1) in a 200 mL beaker containing the resultant solution. The suspension was sonicated for 40 min in order to guarantee a uniform mixing. Next, the suspension was agitated for another half hour after 0.5 M potassium hydroxide (KOH) was added dropwise. After that, a 10 mL/L hydrazine solution was added to the mixture, and the reduction reaction was started by stirring it for 20 min. The effective integration of CuO nanoparticles into the GO sheets occurred after the addition of hydrazine. After removing contaminants by centrifuging the resultant product at 4000 rpm, it was repeatedly cleaned with DI water. The cleaned material was then placed in the oven and heated to 200°C in order to exfoliate it and improve its effectiveness.

Photocatalytic experiments

All photocatalytic tests were performed in 500 mL photo-reactor made up of quartz glass. 257 W visible light lamp with an intensity of 20 W/m2 was utilized for irradiation purpose. Reaction assembly has appropriate cooling systems of water channels to avoid excess heat produced during the photocatalytic examinations. Nonstop purging of air has been done to the reaction mixture during the treatment process. Centrifugation was utilized for separation of photocatalyst from irradiated solution.

Characterization techniques

The physicochemical characteristics of materials were assessed using a variety of methods. Crystallinity of nanoparticles and nanocomposites was investigated using an X-ray diffraction-7000-Shimadzu Scientific Instrument (Cu-Kα, λ=0.154060 nm). To investigate the physical morphology and microstructure of nanoparticles and nanocomposites, a field emission scanning electron microscope (FE-SEM, S-4800 Hitachi Ltd., Japan) was utilized at an acceleration voltage of 200 kV. Furthermore, atomic force microscopy (AFM, 550, Agilent, Santa Clara, CA, USA) was employed to generate 3-D surface images. The optical properties of the samples were analyzed using a UV/Visible spectrometer (Lambda 35 Perkin-Elmer), which measured absorbance and bandgap energy over a wavelength range of 200-700 nm at room temperature.

Photocatalytic degradation studies

The efficiency of the GO-CuO nanocomposite in the photocatalytic degradation of Vancomycin, Doxycycline and Clindamycin antibiotics High Performance Liquid Chromatography (HPLC) measurements was evaluated by monitoring the maximum absorption wavelength (λmax) of the Vancomycin, Doxycycline and Clindamycin antibiotics drugs(15 mg/L) at 358 nm under sunlight exposure. To begin the degradation process, a 15 mL solution of Vancomycin, Doxycycline and Clindamycin antibiotics drug was prepared in a volumetric flask, followed by the addition of 8 mg/L of the prepared photocatalyst to achieve adsorption-desorption equilibrium.

About 1 mL of the sample was homogenized with 5 mL of high-purity Milli-Q water. On 1 mL of 0.5 M tetrabutylammonium hydrogen sulphate solution and 2 mL of sodium carbonate buffer (0.25 M, pH=10.0) were added to 1 mL of the homogenate samples in a Polypropylene (PP) tube and thoroughly mixed for extraction. 5 mL of Methyl Tert-Butyl Ether (MTBE) was added to the prepared mixture and shaken for 20 min. The organic and aqueous layers were separated by centrifugation, and an exact volume of MTBE (4 mL) was removed from the solution. The aqueous mixture was rinsed with MTBE and separated twice; both the rinses were combined in a second PP tube. The solvent was evaporated under nitrogen and replaced with 0.5 mL of methanol. This extract was passed through a nylon mesh filter (0.2 µm) into a HPLC vial. The extraction blanks were prepared using Milli-Q water.

The percentage of photocatalytic degradation was then calculated using Equation (1).

$$(\%)Degradation = X_i - \frac{X_f}{X_i}\, x\, 100 \qquad (1)$$

Where; Xi and Xf are the initial and final concentration of the of the Vancomycin, Doxycycline and Clindamycin antibiotics drug.

When the catalyst absorbs a hv with energy equal to or greater than its band gap, an e- - h+ pair is generated. So, the band gap energy is critical for this process, too wide or too narrow band gap will be ineffective for photocatalysis. When the band gap of the catalyst is too wide, the light irradiation can only induce a few or even no e transition from valence band to conduction band. Although, the generated e- - h+ pair has strong oxidizing-reduction ability, its efficacy for contaminant removal is limited due to the small quantity. With the band gap narrowing, the quantity of e- - h+ pairs are raised. However, when the band gap

is too narrow, the efficacy is reduced because the oxidizing-reduction ability of e- - h+ pair is too weak even though its quantity is increased. Thus, a suitable band gap of the GO and GO-CuO nanocomposite catalyst is essential for its photocatalysis efficiency [63].

Once generated, the e- - h+ pair will separate into a free e- and a free h+. The h+ in the valence band has high oxidation capacity which can degrade Vancomycin, Doxycycline and Clindamycin antibiotics directly [64]. In addition, h+ reacts with H2O in the solution and produces OH● radicals which also have a well-known degradation ability for a wide range of organic compounds through an H-atom abstraction to form water. However, in the case of Vancomycin, Doxycycline and Clindamycin antibiotics, all H atoms have been replaced by F-atoms in the carbon chain, thus Vancomycin, Doxycycline and Clindamycin antibiotics are inert to OH● attack (kOH●+PFOA ≤ 105 1/M.s) [65]. Therefore, the less transformation from h+ to OH● occurs in the photocatalytic system, the better efficacy will be achieved for Vancomycin, Doxycycline and Clindamycin antibiotics degradation. Besides, e- moves to the surface of the catalyst and reacts with adsorbed water to form hydrated electrons (eaq-). Vancomycin, Doxycycline and Clindamycin antibiotics molecules adsorbed on the GO and GO-CuO nanocomposite catalyst surface can be attacked by the eaq- and degraded into shorter-chain compounds [66].

Measurements of Vancomycin, Doxycycline and Clindamycin Antibiotics

Sample preparation

Before commencing the sample preparation, 50 µL of Milli-Q water was added to the patient samples [67]. To prepare the CSs, QCs, and patient samples for analysis, 500 µL of extraction solution (composed of 50% methanol, 50% Milli-Q water, and 1% formic acid) was added to extract clindamycin, Doxycycline and Vancomycin from the aquatic samples. Subsequently, 500 µL of the working solution ISTD was added to each sample. The samples were vortexed for approximately 60 seconds and centrifuged for 5 min at 1811 g, respectively. After centrifugation, 50 µL of the supernatant was transferred to an autosampler vial along with 200 µL of eluent A. After mixing, the extracts were injected into a Waters Xevo TQ-S Micro UHPLC-MS/MS system for analysis.

Chromatographic- and Mass-Spectrometry Conditions

Instrumentation

The analyses were conducted using a Waters Acquity UHPLC-MS/MS system (Waters Corp., Milford, MA). The UHPLC system was linked to a Waters TQ-S micro mass spectrometer equipped with a triple quadrupole and an Electrospray Ionization (ESI) probe. The setup also included an acuity binary solvent manager, sample manager, and column manager. Data processing was performed using Masslynx V4.1 and Targetlynx V4.1 software.

Chromatographic conditions

For chromatographic separation and optimization, a Waters Acquity UHPLC HSS T3 C18 column (1.8 µm, 2.1 × 100 mm) was used at a column temperature of 45°C. The mobile phase consisted of eluents A and B. Eluent A consisted of 0.1% formic acid and 2 mM ammonium acetate in 1 L of Milli-Q water, and eluent B consisted of 0.1% formic acid and 2 mM ammonium acetate in 1 L of LC-MS-grade methanol. The gradient profile was as follows: starting with 95% eluent A and 5% eluent B for the initial 0.80 min, transitioning to 10% eluent A and 90% eluent B over 2 min, and finally returning to 95% eluent A and 5% eluent B for the remaining 2.4 min. The total analytical runtime per sample was 5.2 min. Linear gradient elution at a constant flow rate of 0.35 mL/min was employed. Injection volumes were set at 1 and 10 µL for Clindamycin, and Vancomycin for bone samples and at 10 µL for both Doxycycline, Clindamycin as Vancomycin for samples. The autosampler temperature was maintained at +15°C. The seal wash was performed using a water-methanol mixture (9:1), with methanol serving as the needle wash.

Mass-spectrometry conditions

The ideal mass spectrometry (MS) conditions were established for each compound during the method development process. The MS conditions were operated using electrospray ionization in the positive mode (ESI+). Each analyte was prepared in a methanol solution at a concentration of 1 mg/L and directly infused into the MS/MS system. The cone voltage and collision energy were optimized individually for each analyte. The optimal MS settings were as follows: a capillary voltage of 3.0 kV, a cone voltage of 20 V, a desolvation temperature heated at 400°C with a desolvation gas flow rate of 500 L/h, and a cone gas flow rate of 10 L/h. The optimized conditions for each analyte are listed in Table 1.

Compound	Parent ion (m/z)	Product ion (m/z)	Cone Voltage (V)	Collision Energy (eV)	Retention Time (min)
Clindamycin	425.0	125.9	2	38	1.56
Vancomycin	725.6	144.0	14	14	1.16
Doxycycline	731.7	144.1	32	12	1.17

Table 1. Mass Spectrometry Conditions for Clindamycin, Vanco-

mycin and Doxycycline

Method validation

The method described was validated in accordance with the guidelines outlined by the European Medicines Agency (EMA) and the US Food and Drug Administration (FDA) for bioanalytical method validation, as detailed in the guidelines of 2011 and 2018, respectively. Validation procedures were conducted to ensure the linearity, accuracy, precision, carry-over, and stability of both antibiotics in both matrices. These values met the requirements based on the guidelines of the EMA and FDA; therefore, this method was used to measure the concentrations of vancomycin and clindamycin in synovial tissue and bone of patients with PJI.

Linearity

The linearity of the method was validated by constructing a calibration curve comprising known concentrations in duplicates. This process included measuring a blank sample without an ISTD and a zero sample with an ISTD. After applying a weighting factor of 1/x, the response (the peak area of each CS divided by the peak area of the ISTD) was plotted against the theoretical concentrations. Linear least-squares regression was employed to analyze linearity, with the determination coefficient (r2) required to be at least 0.990 for each calibration curve.

LLOQ and ULOQ

The lower Limit of Quantification (LLOQ) and Upper Limit of Quantification (ULOQ) were established. The LLOQ, which represents the lowest standard of the calibration curve, was measured 5 times on 3 separate days. The LLOQ experiments were based on QCs. Accuracy and precision were required to fall within the accepted values (80-120%). The ULOQ is defined as the highest CS. The deviation from the calibration curve was required to be less than 15%.

Accuracy and precision

Intraday precision was assessed by measuring 3 different concentrations, quality control-low (QC-L), Quality Control-Medium (QC-M), and Quality Control-High (QC-H), 5 times within a single run. Interday precision and accuracy were also evaluated by measuring QC-L, QC-M, and QC-H 5 times on 3 different days. For precision, the relative SD (RSD) should be <15%. The accuracy was evaluated based on the bias from the measured value compared with the nominal value, and these deviations should be lower than 15%.

Carry-over effect

To assess the carry-over effect, a blank sample containing ISTD was measured immediately after the ULOQ. The carry-over effect was considered acceptable if it was < 20% of the LLOQ.

Stability

The autosampler stability was assessed by storing the extracts of the QC samples at low, medium, and high concentrations in the autosampler at 15°C for 24 h. Subsequently, the extracts were analyzed in duplicate and against freshly prepared CSs. The concentrations measured after 24 h were compared with those measured initially (T=0), with acceptable recoveries within ±15%.

Measurements of sun light powers

The low sun light powers were measured at between 8.00-9.00 a.m hours in August by an Merck Luminimeter. The high sun light powers were measured at between 11.00-14.00 pm hours in the same month while the mean sun light powers were muasured at between 17.00-18.30 p.m

Results And Discussıons

XRD analysis of GO and GO-CuO nanocomposite

The XRD is an effective analytical tool that is being broadly used for the determination of size and crystalline structure of material. For the determination of crystalline structure and size of as-synthesized GO-CuO nanocomposite, GO and CuO nanoparticles the XRD was successfully used. The exceptional crystallinity of the fabricated CuO nanoparticles identified as a monoclinic phase matching JCPDS card 45.0937, is clearly evidenced by their XRD patterns. The strong reflection observed at (002), further reinforced by the presence of peaks at (002), (111), (-202), (202), (-113), and (-311), demonstrate the formation of a highly ordered crystalline structure, as shown in Figure 1. The XRD diffraction patterns of GO and GO-CuO nanocomposite, are shown in Figure 2. The 001 pattern clearly manifested that the GO has been successfully prepared, while the 002 patterns in CuO with other reported patterns such as 110, 002, 111, −202, 020, 202, −113, and −311 clearly showed that the CuO has been prepared and the GO is successfully reduced to the GO. Moreover, the size of the GO-CuO nanocomposite is also calculated as 43.7 nm by using the Debye-Scherrer equation. In addition, all diffraction patterns highlight that the GO-CuO nanocomposite has a crystalline nature.

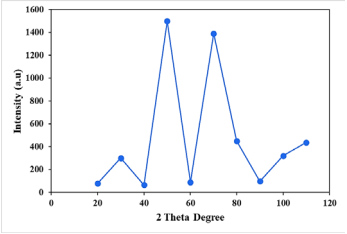

Figure 1. XRD pattern of CuO

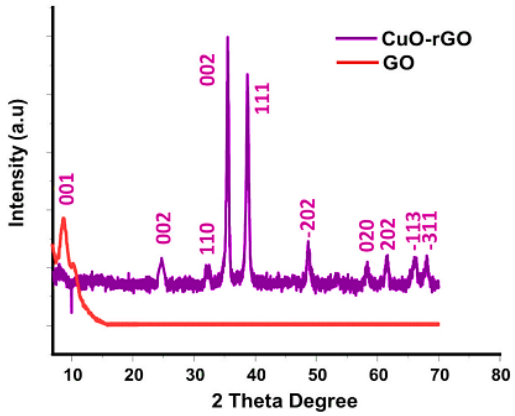

Figure 2. XRD diffraction pattern of GO-CuO nanocomposites and GO showing high crystalline structure.

Determination of morphological texture of GO and GO-CuO nanocomposite

The SEM studies were carried out for the as-prepared GO-CuO nanocomposite and compared with pure GO and CuO nanoparticles (Figure 3a,3b). The SEM image revealed that the CuO NPs consists of diminutive particles exhibiting a nanoflake-like architecture, coupled with a highly porous surface. Moreover, the SEM images of GO and GO-CuO nanocomposites are shown (Figure 3a,3b), respectively. The SEM image of GO confirms its successful preparation, displaying thick sheets. The SEM image of the GO-CuO nanocomposite reveals the uniform distribution of CuO nanoparticles (Figure 3c) within the GO st in surface area and exfol them more effective for de

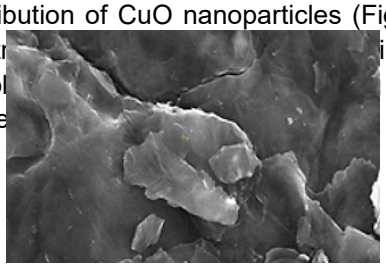

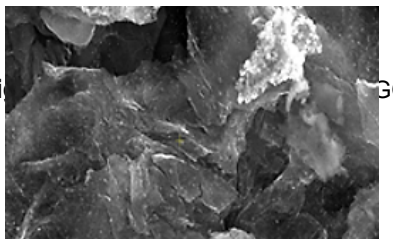

Fi GO-CuO

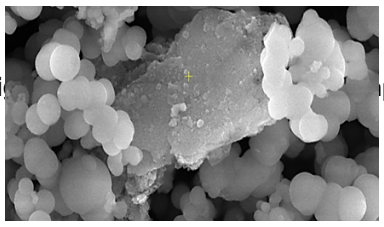

Fi posite

Figure 3c. SEM images of CuO nanocomposite

Elemental analysis of GO-CuO nanocomposite

For the determination of purity and elemental composition of materials, EDX is widely used. For the determination of elemental percentages of elements in the prepared GO-CuO nanocomposite, an EDX instrument was used. The elemental percentage of GO-CuO nanocomposite is shown (Figure 4). The percentages of elements in prepared GO-CuO nanocomposites are determined as C 52.10%, Cu 23.30%, O 21.80%, and with little existence of Cl as 2.80% (Table 2). The EDX analysis clearly showed that the as-synthesized GO-CuO nanocomposite is highly pure and impurity-free. This purity will increase the performance of material in different analytical applications.

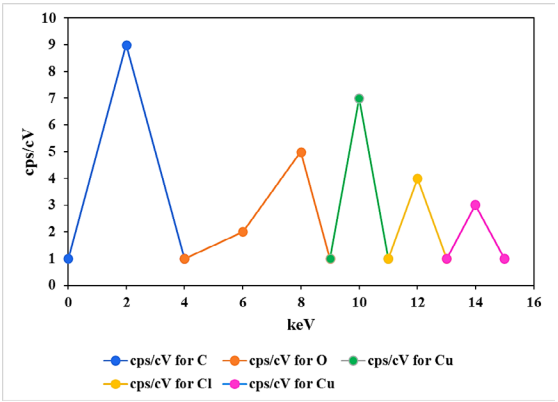

Figure 4. EDX analysis ofGO/CuO nanocomposite with C, Cu and O

	Wt (%)	ó
C	52.1	0.55
Cu	23.3	0.45
O	21.8	0.44
Cl	2.8	0.1

Table 2. The percentages of elements in prepared GO-CuO nanocomposite

3D Morphological analysis of GO-CuO nanocomposite

AFM is a highly sensitive and effective analytical tool being broadly exploited for the determination of size and 3D morphological texture of materials. To evaluate the size and 3D texture of the GO-CuO nanocomposite, an AFM instrument was employed as displayed (Figure 5). The particles of CuO are seen to be embossed on the surface of GO. These particles exist like little islands that clearly display that the particles of CuO have been successfully introduced into the sheets of GO. The AFM instrument also calculated the average size of the as-prepared GO-Cu O nanocomposite. The maximum size of GO-CuO nanocomposite was determined to be up to 25 nm, which is in good

agreement with the size calculated by XRD.

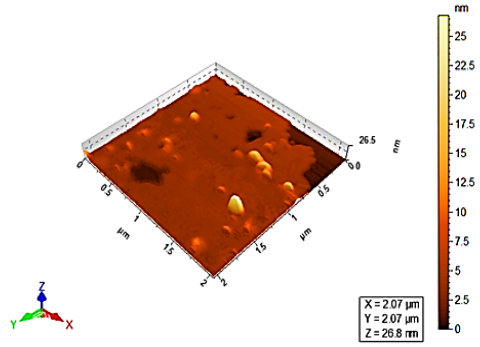

Figure 5. AFM analysis of GO-CuO nanocomposite with the maximum size of 25 nm

Photocatalytic performance of GO-CuO nanocomposite for Vancomycin, Doxycycline and Clindamycin antibiotics

The degradation of performance of prepared GO-CuO nanocomposite for the Vancomycin, Doxycycline and Clindamycin antibiotics were evaluated by UV-visible spectrophotometer. The degradation efficiency of as prepared GO-CuO nanocomposite was further enhanced by optimizing certain conditions, e.g., usage of the proton source sodium borohydride (NaBH4), the exploitation of sunlight, and the catalyst dose. The maximal UV-visible peak of Vancomycin, Doxycycline and Clindamycin antibiotics were monitored around 399-401 nm (Figure 6).

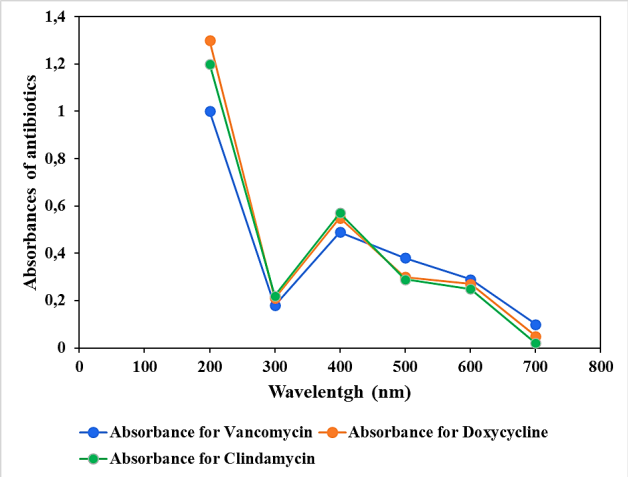

Figure 6. UV-visible peaks of Vancomycin, Doxycycline and Clindamycin antibiotics

Effects of Operational Conditions on the Photoremoval Yields of Vancomycin, Doxycycline and Clindamycin Antibiotics

Effect of GO-CuO catalyst doses on the yields of the Vancomycin, Doxycycline and Clindamycin antibiotics

In the beginning of the studies in order to detect the maximal photodegradation yields of the aforementioned antibiotics some optimal operational conditions were choosen from the recent literature [69-71]. The effects of increasing GO-CuO catalyst concentrations (0.2 mg/L, 0.5 mg/L, 1.0 mg/L, 2.0 mg/L and 3.0 mg/L) on the photoremoval yields of Vancomycin, Doxycycline and Clindamycin antibiotic yields were investigated at 7 min sun light exposure durations, at 1.0 mg/l GO-CuO nanocomposite concentration, at pH=7.0 and at 30°C, respectively (Figure 7).

52.79%, 75.10%, 92.74% and 85.46% Vancomycin photoremoval efficiencies were obtained at 0.2 mg/L, 0.5 mg/L, 2.0 mg/L and 3.0 mg/L GO-CuO catalyst concentrations, respectively, after 7 min sun light exposure duration, at pH=7.0, at 30°C, respectively (Figure 7). Maximum 99.00% Vancomycin photoremoval yield was found at 1.0 mg/L GO-CuO catlysao soncentration, after 7 min sun light exposure duration, at pH=7.0 and at 30oC, respectively (Figure 7). 52.54%, 75.02%, 92.49% and 85.21% Doxycycline photoremoval efficiencies were observed at 0.2 mg/L, 0.5 mg/L, 2.0 mg/L and 3.0 mg/L GO-CuO catalyst concentrations, respectively, after 7 min sun light exposure duration, at pH=7.0, at 30°C, respectively (Figure 7). Maximum 98.70% Doxycycline photoremoval yield was measured at 1.0 mg/L GO-CuO catalyst doses concentration, fter 7 min sun light exposure duration, at pH=7.0 and at 30oC, respectively (Figure 7). 52.65%, 75.08%, 92.58% and 85.40% Clindamycin photoremoval efficiencies were measured at 0.2 mg/L, 0.5 mg/L, 2.0 mg/L and 3.0 mg/L GO-CuO catalyst concentrations, respectively,ation, after 7 min sun light exposure duration, at pH=7.0, at 30°C, respectively (Figure 7). Maximum 98.90% Clindamycin photoremoval yield was obtained at 1.0 mg/L GO-CuO catalyst concentration, after 7 min sun light exposure duration, at pH=7.0 and at 30oC, respectively (Figure 7).

In this study, at 1.0 mg/l nanocomposite concentration maximum 98.90% Clindamycin, 98.70% Doxycycline and 99.00% Vancomycin. As the catalyst dose was increased, a reduction in the Vancomycin, Doxycycline and Clindamycin antibiotic yields were detected (Figure 7). In other words, the further increase in the catalyst dose affect sligtly the photoremoval efficiencies of the aforementioned antibiotics. At low nanocomposite concentrations the treatment costs minimized under sun light. This provides very effective yields for the degradation of Vancomycin, Doxycycline and Clindamycin antibiotics.

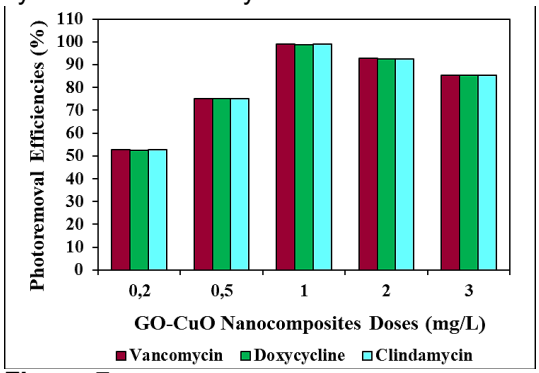

Figure 7. Effect of GO-CuO catalyst doses on degradation of Vancomycin, Doxycycline and Clindamycin antibiotics

At high nanocomposite concentrations sligtly lower photodegradation yields was detected due to turbidity problem. This decrease the photodegradation yields of antibiotics by blocking the active points on the surface of nanocomposite. This cause to decreasing of light intensity in the nanocomposite - antibiotic matrix resulting in low OH● and O2● radical productions. Under optimal nanocomposite doses, the nanocomposite has good agglomeration properties due to its high surface energy by generation sufficient radicals increasing the photodegradation yields. Therfore at optimal nanocomposite concentrations excellent photocatalytic yields was detected in this study.

A significant statistical correlation between the photodegradation efficiency and nanocomposite concentration was found up to an optimal nanocomposite concentration is attained (f=0.02, R2=0.99). After 1.0 mg/l nanoconposite concentration the correlation for a fore mentioned matrix decreased (f=0.11, R2=0.96). In this stdy it was found that the catalyst dose plays a very crucial role in the degradation of antibiotic molecules; by providing electrons from the sun light and effectively photodegraded the Vancomycin, Doxycycline and Clindamycin antibiotics.

Effect of Vancomycin, Doxycycline and Clindamycin antibiotic doses on the photodegradation of Vancomycin, Doxycycline and Clindamycin antibiotics

Effect of increasing Vancomycin, Doxycycline and Clindamycin antibiotic concentrations (300, 500, 1000, 2000, 3000 and 4000 mg/L) on the photodegradation yields of Vancomycin, Doxycycline, and Clindamycin photoremovals was investigated at 7 min sun light exposure duration, at 1.0 mg/L GO-CuO nanocomposite concentration, at pH=7.0, and at 30oC, respectively (Figure 8).

50.42%, 73.64%, 88.53%, 91.25% and 82.77% Vancomycin photodegradation removals were observed at 300, 500, 1000, 2000 and 4000 mg/L Vancomycin concentration, respectively (Figure 8). 99.00% maximum Vancomycin photoremoval yield was found at 3000 mg/L Vancomycin concentration, after 7 min sun light exposure duration, at 1.0 mg/L GO-CuO nanocomposite concentration, at pH=7.0, and at 30oC, respectively (Figure 8).

50.08%, 73.24%, 88.19%, 91.04% and 82.18% Doxycycline photodegradation removals were obtained at 300, 500, 1000, 2000 and 4000 mg/L Doxycycline concentration, after 7 min sun light exposure duration, at 1.0 mg/L rGO-CuO nanocomposite concentration, at pH=7.0, and at 30oC, respectively (Figure 8). 98.70% maximum Doxycycline photoremoval yield was measured at 3000 mg/L Doxycycline concentration, after 7 min sun light exposure duration, at 1.0 mg/L rGO-CuO nanocomposite concentration, at pH=7.0, and at 30oC, respectively (Figure 8).

50.34%, 73.57%, 88.37%, 91.18% and 82.56% Clindamycin photodegradation removals were observed at 300, 500, 1000, 2000 and 4000 mg/L Clindamycin concentration, after 7 min sun light exposure duration, at 1.0 mg/L rGO-CuO nanocomposite concentration, at pH=7.0, and at 30oC, respectively (Figure 8). 98.90% maximum Clindamycin photoremoval yield was found at 3000 mg/L Clindamycin concentration, after 7 min sun light exposure duration, at 1.0 mg/L rGO-CuO nanocomposite concentration, at pH=7.0, and at 30oC, respectively (Figure 8).

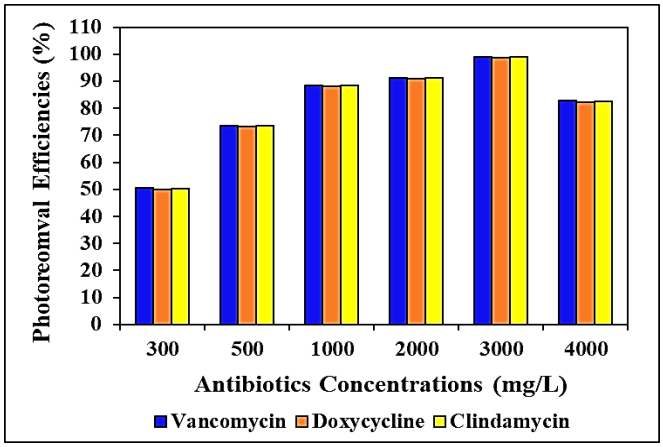

Figure 8. Effect of Vancomycin, Doxycycline and Clindamycin antibiotic doses on degradation of vancomycin, doxycycline and clindamycin antibiotics

A significant statistical linear correlation between the photodegradation efficiency and antibiotic concentration was found up to an optimal nanocomposite concentration is attained at 3000 mg/L antibiotic concentrations. (f=0.023, R2=0.99). Increasing of Vancomycin, Doxycycline and Clindamycin antibiotic concentrations from 300 mg/L up to 3000 mg/L increased the photodegradation yields of all antibiotics (Figure 8). This may be due to the almost all antibiotics (Vancomycin, Doxycycline and Clindamycin) photocatalyzed by GO-CuO nanocomposites and the establishment of equilibrium between the GO-CuO nanocomposites and antibiotics occurred. At 3000 mg/L Vancomycin, Doxycycline and Clindamycin concentrations maximal antibiotic yields were detected at 1.0 mg/l GO-CuO nanocomposite dose. Further increase of all antibiotic concentration up to 4000 mg/l decreased sligtly the antibiotic yields. At this antibiotic dose, a part antibiotics unabsorbed to nanocomposite and remained in the solution. The loading amount of pollutants is a significant factor in the photocatalytic degradation process, because the efficiency could be strongly affected by the number of active sites and photo adsorption ability of the catalyst used. However, it was observed that above a certain optimum antibiotic mass, the yield decrease was not significant.

Effect of proton concentrations on degradation of Vancomycin, Doxycycline and Clindamycin antibiotics

In this study NaBH4 was used as a proton source. Effect of increasing proton (NaBH4) concentrations (0.001, 0.002, 0.003 and 0.004 M) on the photooxidation yields of Vancomycin, Doxycycline and Clindamycin antibiotics were investigated with GO-CuO nanocomposites (Figure 9).

78.54%, 92.47% and 88.21% Vancomycin antibiotic photoremoval efficiencies were obtained at 0.001, 0.003 and 0.004 M proton concentrations, respectively, at pH=7.0 and at 30oC, respectviely (Figure 9). Maximum 99.00% Vancomycin antibiotic photoremoval yield was found at 0.002 M proton concentration, at pH=7.0, at 30oC (Figure 9).

75.11%, 92.24% and 88.15% Doxycycline antibiotic photoremoval efficiencies were observed at 0.001, 0.003 and 0.004 M proton concentrations, respectively, at pH=7.0 and at 30oC, respectviely (Figure 9). Maximum 98.70% Doxycycline antibiotic photoremoval yield was measured at 0.002 M proton concentration, at pH=7.0, at 30oC (Figure 9).

76.63%, 92.35% and 88.19% Clindamycin antibiotic photoremoval efficiencies were obtained at 0.001, 0.003 and 0.004 M proton concentrations, respectively, at pH=7.0 and at 30oC, respectively (Figure 9). Maximum 98.90% Clindamycin antibiotic photo removal yield was found at 0.002 M proton concentration, at pH=7.0, at 30oC (Figure 9).

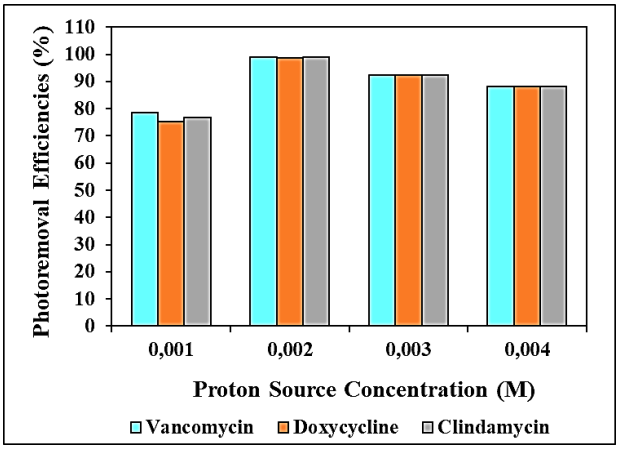

Figure 9. Effect of proton concentrations on degradation of Vancomycin, Doxycycline and Clindamycin antibiotics

A significant statistical linear correlation between the photodegradation efficiency an dproton concentrations for all antibiotics was found up to an optimal proton concentration is attained at 0.02 mg/L (f=0.021, R2=0.99). In the degradation of organic molecules such as dyes and antibiotics, the effective proton plays a very important role, which effectively provides a proton source from certain reducing agents, e.g., NaBH4. In the current experimental study, NaBH4 is used as an effective proton source. To determine the effective results of the proton concentration to antibiotic phtodegradation yields, a fresh solution of 0.002 M NaBH4 was prepared. The effective photodegradation yields of Vancomycin, Doxycycline and Clindamycin antibiotics were observed at 0.002 M NaBH4 concentration and this proton concentration was optimized for further experimental studies (Figure 9).

Effect of sun light ırradiation time on degradation of Vancomycin, Doxycycline and Clindamycin antibiotics

The photoreactor was operated at increasing sun light exposure durations (2, 5, 7, 9 and 12 min) to determine tha pharmaceutical yields at 0.002 M proton source concentration, at pH=7.0, at 30°C, respectively (Figure 10).

58.33%, 74.20%, 93.25% and 87.41% Vancomycin antibiotic photoremoval yields were measured at 2, 5, 9 and 12 min sun light exposure durations, respectively, (Figure 10). 99.00% maximum Vancomycin photoremoval yield was measured at 7 min sun light exposure duration, at 0.002 M, at pH=7.0, at 30oC, respectively (Figure 10).

58.27%, 74.14%, 92.16% and 86.96% Doxycycline antibiotic photoremoval yields were obtained at 2, 5, 9 and 12 min sun light exposure durations, respectively, at 0.002 M proton source concentration, at pH=7.0, at 30°C, (Figure 10). 98.70% maximum Doxycycline photoremoval yield was measured at 7 min sun light exposure duration, at 0.002 M, at pH=7.0, at 30°C, respectively (Figure 10).

58.30%, 74.18%, 92.71% and 87.09% Clindamycin antibiotic photoremoval yields were observed at 2, 5, 9 and 12 min sun light exposure durations, respectively, at 0.002 M proton source concentration, at pH=7.0, at 30°C, (Figure 10). 98.90% maximum Clindamycin photoremoval yield was found at 7 min sun light exposure duration, at 0.002 M, at pH=7.0, at 30°C, respectively (Figure 10).

A significant statistical linear correlation between the photodegradation efficiency and time was found up to an optimal time of 7 min is attained (f=0.023, R2=0.99).

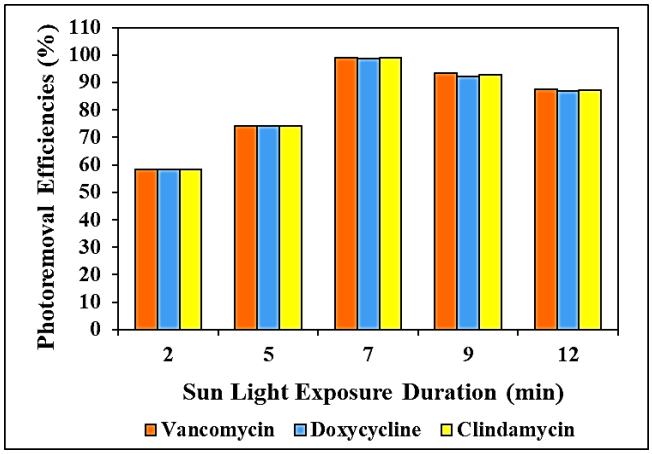

Figure 10. Effect of sun light exposure duration on degradation of Vancomycin, Doxycycline and Clindamycin antibiotics

As the photo oxidation times were increased from 2 min up to 7 min the Vancomycin, Doxycycline and Clindamycin antibiotic yields increased from around 58.27% up to 99.00% under sun light. Further increase of time sligtly decrease the all antibiotic yields after 9 and 12 min photooxidation time. The yields were recorded around 88% and 81% for the aforementioned long photodegradation times for all antibiotics. Data obtained from this study showed that the pharmaceutical yields at longer retention time was sligtly low. In elevated contact times sligtly low OH● radicals production was achieved. Low conversion rates were observed at very short residence times. Althougth, prolonged light irradiation is expected to accelerate the photodegradation of pharmaceutical molecules onto the photocatalyst surface before reaching equilibrium in this study 7 min has enhanced the yields. It can be speculated that the number of electrons transferring from the VB to the CB increases that enhance the amount of electron-hole pairing at 7 min. The optimum illumination time for maximum removal of pharmaceuticals (Vancomycin, Doxycycline and Clindamycin) was obtained as 7 min.

Effect of pH values on degradation of Vancomycin, Doxycycline and Clindamycin antibiotics

The effects of increasing pH values (pH=4.0, pH=7.0, pH=8.0 and pH=11.0) on the yields of antibiotics namely Vancomycin, Doxycycline and Clindamycin were investigated at 0.003 M proton concentration, after 7 min sun light exposure duration, at 1.0 mg/L GO-CuO catalyst concentration, and at 30°C temperature, respectively (Figure 11).

78.65%, 94.06% and 87.24% Vancomycin photoremoval efficiencies was measured at pH=4.0, at pH=8.0 and at pH=11.0, respectively, for the operational conditions given above (Figure 11). Maximum 99.00% Vancomycin photoremoval yield was detected at pH=7.0, at 0.002 M proton souırce concentration, after 7 min sun light exposure duration, at 1.0 mg/L GO-CuO catalyst concentration and at 30°C temperature, respectively (Figure 11).

78.14%, 93.79% and 87.08% Doxycycline photoremoval efficiencies was found at pH=4.0, at pH=8.0 and at pH=11.0, respectively, after 7 min sun light exposure duration, for the operational conditions mentioned above (Figure 11). Maximum 98.70% Doxycycline photoremoval yield was observed at pH=7.0, at 0.003 M proton concentration, after 7 min sun light exposure duration, at 1.0 mg/L GO-CuO catalyst concentration and at 30oC temperature, respectively (Figure 11).

78.46%, 93.91% and 87.17% Clindamycin photoremoval efficiencies was detected at pH=4.0, at pH=8.0 and at pH=11.0, respectively, at 0.003 M proton souırce concentration, after 7 min sun light exposure duration, at 1.0 mg/L GO-CuO catalyst concentration and at 30oC temperature, respectively (Figure 11). The maximum 98.90% Clindamycin photoremoval yield was obtained at pH=7.0, at 0.003 M proton concentration, after 7 min sun light exposure duration, at 1.0 mg/L GO-CuO catalyst doses concentration and at 30°C temperature, respectively (Figure 11).

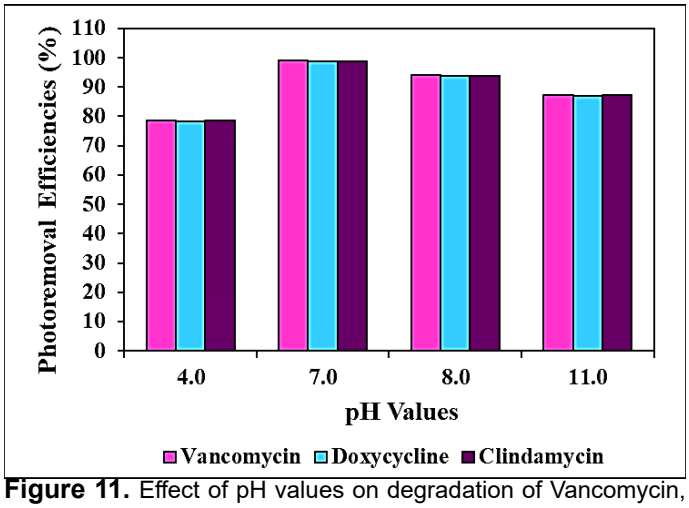

Figure 11. Effect of pH values on degradation of Vancomycin, Doxycycline and Clindamycin antibiotics

A significant statistical linear correlation between the photodegradation efficiency and Ph values was found up to an optimal pH of 7.0 is attained (f=0.023, R2=0.99).

The results indicate that with changing the pH of the solution media, the acid-base property at surface of the photocatalyst was remarkably influenced the photodegradation performance of the nanomaterial. The electrostatic based repulsion between the deprotonated GO-CuO nanocomposites and hydroxide ion (OH-) is the possible cause for the observed increase in performance of the pharmaceuticals at pH=7.0, because the repulsion improve the formation of OH● radicals that consequently increase the photocatalytic efficiency of GO-CuO nanocomposites. At pH values > 7.0 and < 7.0, the decomposition of pharmaceuticals becomes even more hindered, which could be explained by the reduced sorption possibility of the cationic pharmaceuticals at the GO-CuO nanocomposite surface which gained not sufficient positive charges (i.e., due to protonation) on the surface of catalyst causing repulsion.

Effect of temperature on degradation of Vancomycin, Doxycycline and Clindamycin antibiotics

The photoreactor was operated with different temperatures (20,30,40 and 50oC) to determine the photoremoval yields of Vancomycin, Doxycycline and Clindamycin antibiotics at 0.003 M proton concentration, after 7 min sun light exposure duration, at 1.0 mg/L GO-CuO nanocomposite concentration, at pH=7.0, respectively (Figure 12).

80.05%, 92.48% and 75.33% Vancomycin photoremoval efficiencies were measured at 20°C, 40°C and 50°C,

respectively, fort he same operational conditions given above (Figure 12). 99.00% maximum Vancomycin photoremoval yield was found at 30oC, at 0.003 M proton concentration, after 7 min sun light exposure duration, at 1.0 mg/L GO-CuO nanocomposite concentration, at pH=7.0, respectively (Figure 12).

79.73%, 92.09% and 75.08% Doxycycline photoremoval efficiencies were detected at 20°C, 40°C and 50°C, respectively, at 0.003 M proton concentration, after 7 min sun light exposure duration, at 1.0 mg/L GO-CuO nanocomposite concentration, at pH=7.0, respectively (Figure 12). 98.70% maximum Doxycycline photoremoval yields was measured at 30oC, fort he aforementioned operational conditions (Figure 12).

79.84%, 92.37% and 75.29% Clindamycin photoremoval efficiencies were obtained at 20°C, 40°C and 50°C, respectively, at 0.003 M proton concentration, after 7 min sun light exposure duration, at 1.0 mg/L GO-CuO nanocomposite concentration, at pH=7.0, respectively (Figure 12). 98.90% maximum Clindamycin photoremoval yield was observed at 30oC, fort he operational conditions given above (Figure 12).

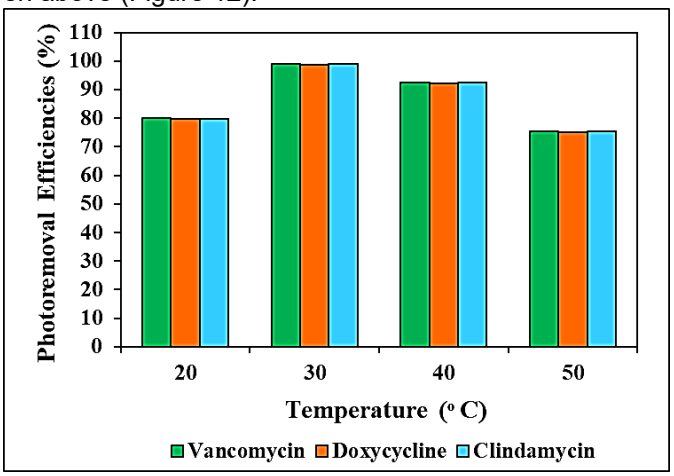

Figure 12. Effect of temperature on degradation of Vancomycin, Doxycycline and Clindamycin antibiotics

A significant statistical linear correlation between the photodegradation efficiency and temperature was found upto an optimal temperature of 30oC is attained (f=0.023, R2=0.99).

In heterogeneous photocatalytic systems, temperature was found to have a significant effect on the photodegradation of pharmaceuticals. In particular, low temperatures favour the adsorption of the pharmaceuticals onto the catalyst, which is a spontaneous exothermic process. Nevertheless, in this case the adsorption of the degradation products is also enhanced, thus reducing the number of active sites on the catalyst. In contrast, high temperatures lead to an increase in the mobility of the pharmaceutical molecules, therefore kinetic energy was increased. However, the enhanced kinetic energy of the pharmaceutical molecules may also allow them to escape from the photocatalyst surface, without being subjected to photodegradation. On the other hand the morphology of the catalyst is very relevant when studying the effect of temperature on the photodegradation of pharmaceuticals. Although, increasing the temperature elevated the photocatalysis yields, a rise in temperature had a negative effect. This was explained due to the super activity of the pharmaceutical surface compared to the nanoparticles.

Effect of sun light powers on degradation of Vancomycin, Doxycycline and Clindamycin antibiotics

Effect of increasing sun light powers (20,40,50 and 60 W/m2) on the photooxidation yields of Vancomycin, Doxycycline, and Clindamycin antibiotics were investigated with 3000 mg/L antibiotic concentration, at 0.003 M proton concentration, after 7 min sun light exposure duration, at 1.0 mg/L GO-CuO nanocomposite concentration, at pH=7.0, and at 30oC, respectively (Figure 13).

82.73%, 95.40% and 84.32% Vancomycin photoremoval efficiencies were obtained at 20, 50 and 60 W/m2 sun light powers, respectively, fort he optimized operational conditions given above (Figure 13). Maximum 99.00% Vancomycin photoremoval yield was detected at 40 W/m2 sun light power, at 3000 mg/L antibiotic concentration, at 0.003 M proton concentration, after 7 min sun light exposure duration, at 1.0 mg/L GO-CuO nanocomposite concentration, at pH=7.0, and at 30oC, respectively (Figure 13).

82.25%, 95.18% and 84.09% Doxycycline photoremoval efficiencies were observed at 20, 50 and 60 W/m2 sun light powers, respectively (Figure 13). Maximum 98.70% Doxycycline photoremoval yield was mesured at 40 W/m2 sun light power, at 3000 mg/L antibiotic concentration, at 0.003 M proton concentration, after 7 min sun light exposure duration, at 1.0 mg/LrGO-CuO nanocomposite concentration, at pH=7.0, and at 30°C, respectively (Figure 13).

82.68%, 95.34% and 84.26% Clindamycin photoremoval efficiencies were obtained at 20, 50 and 60 W/m2 sun light power, respectively, at 3000 mg/L antibiotic concentration, at 0.003 M proton concentration, after 7 min sun light exposure duration, at 1.0 mg/L rGO-CuO nanocomposite concentration, at pH=7.0, and at 30°C, respectively (Figure 13). Maximum 98.90% Clindamycin photoremoval yield was detected at 40 W/m2 sun light power, fort he optimized operational conditions given above (Figure 13).

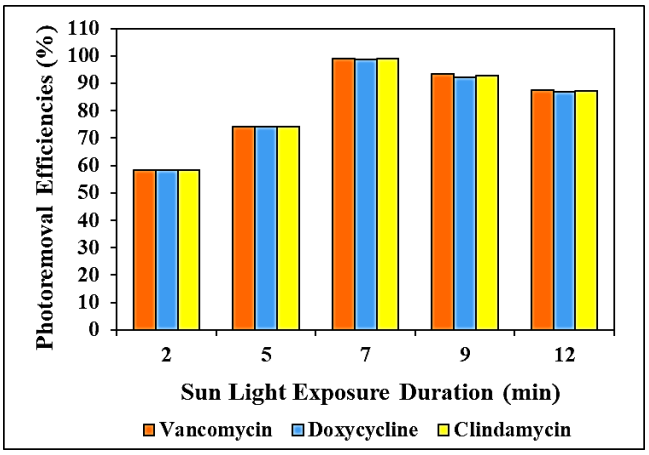

Figure 13. Effect of sunlight powers on degradation of Vancomycin, Doxycycline and Clindamycin antibiotics

A significant statistical linear correlation between the photodegradation efficiency and sun light was found upto an optimal sunlight power of 40 W/m2 is attained (f=0.023, R2=0.99).

Photocatalytic reaction rate depends largely on the radiation absorption of the photocatalyst, where the increase in light intensity enhances the degradation rate and the yield in photocatalytic degradation. At low light intensities (20 W/m2), the photodegradation yields of all antibiotics were low. Further increae of sunlight power to 40 W/m2 would increase linearly the photodegradation efficiencies with increasing light intensity. At intermediate light intensities, above 40 W/m2, the rate would depend on the square root of the light intensity. This is likely, because at low light intensity, reactions involving electron-hole formation are predominant, and electron-hole recombination is negligible. However, at increased light intensities (50-60 W/m2) the, electron-hole pair separation competes with recombination, thereby causing lower effect on the antibiotic photodegradation yields. The enhancement of the photodegradation of Vancomycin, Doxycycline and Clindamycin photoremovals increased as the light intensity increased up to 40 W/m2 (Figure 13).

In the study performed by Jong the Doxycycline removal yields was detected as 82% after 34 min under UV light with 9 mg/L BiVO4-H2O2. 87% Clindamycin photoremoval efficiency was detected with 10 mg/L nano ZnO after 40 min. [70]. 89% Vancomycin removal rates was detected with 20 mg/L nano MnO. 89% and 90% Doxycycline removal efficiencies were detected with 9 mg/L TiO2/Clinoptilic soil and rGO-CuO nanocomposite under UV ligth. In these studies the antibiotic yilds were lower than our study data. It is important to note that the nanocomposite concentrations used in the aforementioned studies were extremely high comapred to our study. Furthermore, in our study sunlight was used instead of UV lumps necessitating high energy. Furthermore, the reusability studies showed that the nanocomposite can be reused 5 times with high yields. These minimize the total cost of the photocatalysis process.

Photodegradation kinetic of Vancomycin, Doxycycline and Clindamycin antibiotics with GO-CuO nanocomposite

For investigation the photodegradation order of the photocatalysis reactions, and rate constants, the maximum reduction and the degradation yields of the Vancomycin, Doxycycline and Clindamycin antibiotics were investigated. The Lagergren kinetic model was used for the pseudo first-order reaction during degradation of Vancomycin, Doxycycline and Clindamycin antibiotics using GO-CuO nanocomposite [27] (Equation 2).

$$(q_e - q) = lnq_e - \frac{k_1 t}{2.303} \qquad (2)$$

Here, k1, qt, and t were the kinetic constants of Vancomycin, Doxycycline and Clindamycin antibiotics and qt is the antibiotic masses photodegraded. By plotting (qe-qt) against time, the intercept, slope, and rate constant k1 were determined.

Pseudo-first-order model for Vancomycin

This model assumes that the rate of drug binding depends on the number of empty spaces left on the surface. By ploting [ln(qe-qt)] on the Y-axis versus time t on the X-axis the kinetic constants can be interpreted (Equation 3) If it is a good fit, the data points will form a straight line with suitable kinetic constants.

$$\ln(q_e - q_t) = lnq_e - k_1 t \qquad (3)$$

Where; qe: Vancomycin amount photodegraded at equlibrium, qt: Vancomycin amount photodegraded at time t, k1: pseudo-first-order rate constants of photodegraded antibiotics, respectively.

Pseudo-second-order model for Vancomycin

This model assumes that the rate of drug binding depends on both the number of empty surface spaces of nanocomposite and the amount of drug already bound. A chemical reaction cbetween the drug and the surface is occurred. By plotting of t/qt on the Y-axis versus time t on the X-axis the intercept can be calculated: A straight line means that the model is a perfect linear fit. qe can be calculated from the slope (which equals to 1/qe) and k2 from the intercept (Equation 4).

$$\frac{t}{q_t} = \frac{1}{k_2 q_e^2} + \frac{1}{q_e} t \qquad (4)$$

Where; k2 is the pseudo second-order rate constant.

By Plotting the equation t/qt versus t the rate constant k2, slope, intercept, and correlation coefficient R2 were calculated.In Figure 14a, 14b the kinetic studies results for the pseudo first-order and the pseudo second-order rate constants during the photodegradation of Vancomycin antibiotics by using GO-CuO nanocomposite were showed.

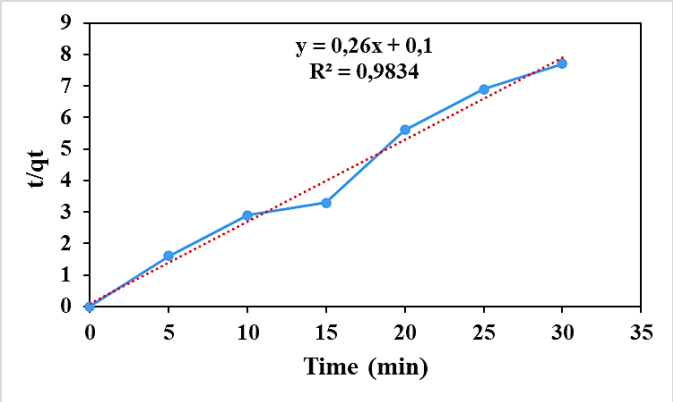

Figure 14a. Kinetic study for the pseudo first-order for the degradation study of Vancomycin antibiotics by using GO-CuO nanocomposite

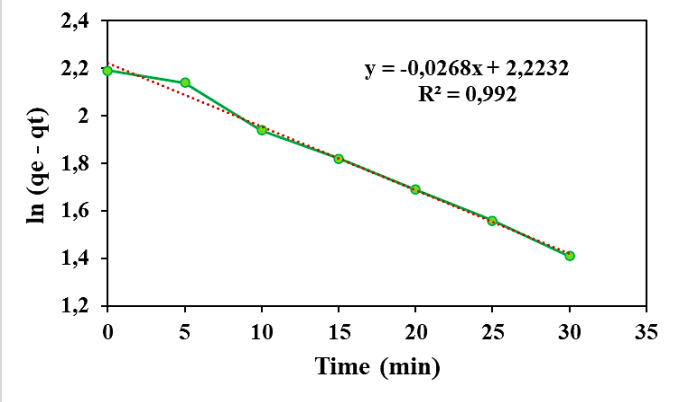

Figure 14b. Kinetic study for the pseudo second-order for the degradation study of Vancomycin antibiotics by using GO-CuO nanocomposite

Pseudo-first-order equation for Doxycycline

The Equation (5) was used in this kinetic model:

$$log(q_e - q) = \log(q_e) - \frac{k_1 t}{2.303} \qquad (5)$$

Where; qe: Amount of Doxycycline photodegraded at equilibrium (mg/g), qt: Amount of Doxycycline photodegraded any time t (mg/g), k1: Pseudo-first-order rate constants of antibiotics during photodegradation(1/min).

Pseudo-second order equation for Doxycycline

The Equation is Eq (6):

$$\frac{t}{q_t} = \frac{1}{k_2 q_e^2} + \frac{1}{q_e} t \qquad (6)$$

In the pseudo-second-order model, by plotting of time (t) on the X-axis and (t/qt) on the Y-axis the R2 was calculated as 0.9931 (Figure 15a, 15b), while k2 represents the rate constant (g/mg.min).

In Figure 15a, 15b the kinetic studies results for the pseudo first-order and the pseudo second-order rate constants obtained from the photodegradation of Doxycycline antibiotics is illustrated by using GO-CuO nanocomposite.

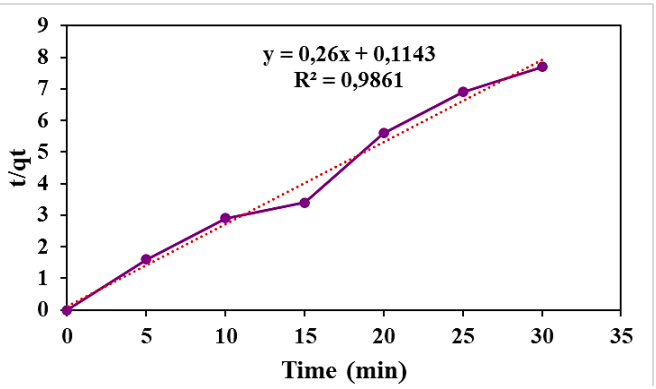

Figure 15a. Kinetic study for the pseudo first-order for the photodegradation kinetic study of Doxycycline antibiotics by using GO-CuO nanocomposite

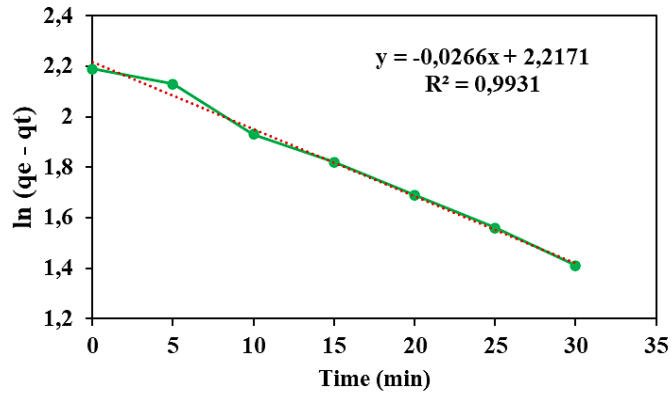

Figure 15b. Kinetic study for the pseudo second-order for the photodegradation kinetic study of Doxycycline antibiotics by using GO-CuO nanocomposite

Pseudo-first-order model for Clindamycin

This model assumes that the rate of the kinetic process is based on the number of available unused sites and it is available when physical forces (physisorption) drive the interaction between antibiotics and nanocomposite (Equation 7):

$$\ln(q_e - q_t) = \ln(q_e) - k_1 t \qquad (7)$$

Where; qe: Amount of Clindamycin at equilibrium (mg/g), qt: amount of Clindamycin at time t (mg/g), k1: pseudo first-order rate constant s of antibiotics(1/min), t: time (min), respectively.

If a plot of ln (qe-qt) on the y-axis versus t on the x-axis gives a straight line this shows that the fit is good. The slope of the line is equal to -k1, and the y-intercept is equal to ln(qe).

Pseudo-second-order model for Clindamycin

This model assumes that the process rate depends on both the amount of Clindamycin on the photocatalyst surface and the amount still available. It often points to chemical bonding (chemisorption) (Equation 8):

$$\frac{t}{q_t} = \frac{1}{k_2 q_e^2} + \frac{1}{q_e} t \quad (8)$$

Where; k2: pseudo second-order rate constant (g/mg.min).; the slope is equal to 1/qe, while the y-intercept is equals to 1/k2.qe2.

The kinetic experiments of pseudo first-order showed that the dots seemed to be away from the straight line, which clearly highlights that the current experiment done for the degradation of Vancomycin, Doxycycline and Clindamycin antibiotics did not follow a pseudo first-order reaction with low kinetic constants. Therefore, the pseudo second-order equation of the Lagergren model was applied by using the same method for the same experimental data by using Equation (9).

$$\frac{t}{q_t} = \frac{1}{k_2 q_e^2} + \frac{t}{q_e} t \quad (9)$$

Plotting the equation t/qt versus t yields the rate constant k2, slope, intercept, and correlation coefficient, where k2 represents the rate constant.

In Figure 16a the kinetic studies for the pseudo first-order and the pseudo second-order rate constants during the photodegradation of Clindamycin antibiotics was shown by using GO-CuO nanocomposite.

(Figure 16b) shows that the pseudo second-order experimental results with slope, intercept, and correlation coefficient of R2=0.9961.

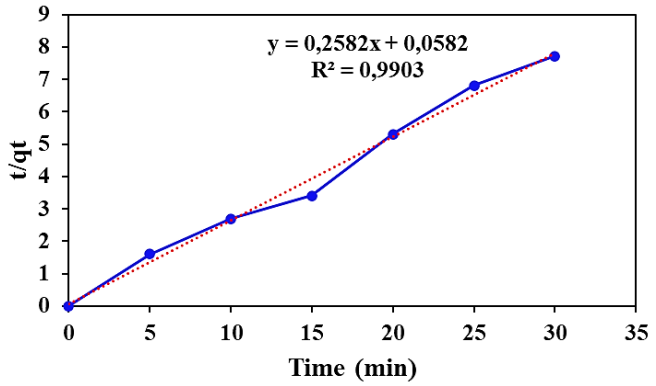

Figure 16a. Kinetic study for the pseudo first-order for the degradation study of Clindamycin antibioticsby using GO-CuO nanocomposite

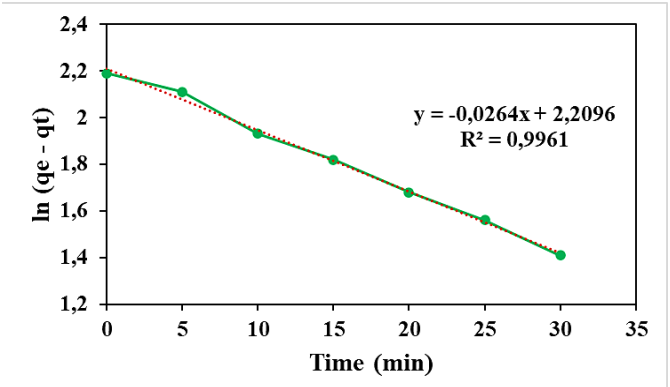

Figure 16b. Kinetic study for the pseudo second-order for the degradation study of Clindamycin antibioticsby using GO-CuO nanocomposite

By observing the the photodegradation kinetic constants and correlation coefficients of the pseudo second-order kinetic model it is seen that all dots in pseudo second-order are seen to be on the linear line and high kinetic constrants of all antibiotics was calculated. Therefore , it can be concluded that the photodegradation reaction model of Vancomycin, Doxycycline and Clindamycin antibiotics followed the pseudo second-order Lagergren model (Table 3).

Antibiotics	Pseudo first-order			Pseudo second-order		
	k1 (1/min)	qe (mg/g)	R2	k2 (mg/min)	qe (mg/g)	R2
Vancomycin	0.00519	0.538	0.9834	0.0281	6.074	0.9920
	intercept	slope		intercept	slope	
	0.1	0.26		2.2232	0.0268	
Doxcycline	0.00452	0.530	0.9861	0.0279	6.071	0.9931
	intercept	slope		intercept	slope	
	0.1143	0.26		2.2171	0.0266	
Clindamycin	0.00432	0.526	0.9903	0.0272	6.069	0.9961
	intercept	slope		intercept	slope	
	0.0582	0.2582		2.2096	0.0264	

Table 3: Kinetic parameters of pseudo first-order and pseudo second-order reactions for Vancomycin, Doxycycline and Clindamycin antibiotic photodegradation with Lagergren Model.

Photodegradation mechanism of Vancomycin, Doxycycline and Clindamycin antibiotics

Vancomycin photodegradation occurs primarily through advanced oxidation pathways where light exposure breaks down the antibiotic's complex glycopeptide structure into smaller, less active fragments. Vancomycin does not degrade easily by direct sunlight alone, but its breakdown accelerates significantly via photosensitized oxidation and photocatalysis. Singlet oxygen (1Δg) pathway is in the presence of specific photosensitizers (like Rose Bengal), light excitation generates singlet oxygen. This active species acts as an electron acceptor, targeting the phenolic groups

in the chemical structure of Vancomycin. This mechanism forms an encountered complex with partial charge-transfer character and is highly favored under alkaline conditions due to the ionization of the phenolic groups. Radical-mediated pathway is when photosensitizers like Riboflavin are active, the degradation switches to a radical-based mechanism via direct interaction with the excited triplet state of the sensitizer. OH● radical attack is in advanced oxidation processes (AOPs) and during photocatalysis highly reactive OH● radicals was occurred. These radicals attack to non-selectively on the vancomycin molecules, leading to mineralization. Because Vancomycin is a large heptapeptide molecule, the oxidative attack yields with specific chemical footprints. Deamination is the breakdown processes systematically and nitrogen-containing groups are stripping from the core peptide structure, resulting in the production of ammonia (NH□). Dechlorination is the chlorinated aromatic rings within the vancomycin framework are vulnerable to photo-induced cleavage, releasing chlorides (Cl□) into the solution. Mineralization is prolonged by sun ligth and ultimately breaks down the remaining carbon skeleton into carbon dioxide (CO□) and water (H□O) by reducing the ecotoxicity of the antibiotic residues.

Doxycycline photodegradation occurs through direct photodegradation process and indirect reactive oxygen species (ROS) pathways. Light absorption triggers structural cleavage, breaking the antibiotic down into smaller, less harmful molecules.

Primary reactive species (the driving forces) are when visible with a photocatalyst strikes the system, it generates highly reactive transient species that attack the Doxycycline molecule. OH● radicals are the most aggressive, non-selective oxidants that attack electron-dense sites. O2- ● radical anions are formed via electron transfer to dissolved oxygen, triggering initial ring cleavage. Photogenerated Holes (h□) are directly oxidize the antibiotic adsorbed onto photocatalyst surfaces.

Main chemical pathways and mechanisms are the chemical structure of Doxycycline undergoes specific functional group alterations during the degradation process. Demethylation is the attacks of radicals causing the removal of methyl groups (-CH3), particularly from the dimethylamino group attached to the antibiotic core. Dehydroxylation is the elimination of hydroxyl (-OH) groups from the phenol and alcohol rings of the antibiotic molecule.s Deamination is cleavage of the amine (-NH2) or dimethylamino carbon-nitrogen bonds, significantly decreasing the antibiotic potency. Ring opening is advanced oxidation by OH● breaks down the multi-ring naphthacene core structure of Doxycycline. Ultimate mineralization is following ring opening, the unstable intermediates continue to fragment into low-molecular-weight organic acids. Eventually, they completely mineralize into harmless inorganic end-products (Equation 10):

$$Doxycycline\ Intermediates \xrightarrow{OH^{\bullet}/O_2^{-\bullet}} CO_2 + H_2O + NH_4^+ + NO_3^- \qquad (10)$$

The photodegradation mechanism of Clindamycin relies primarily on indirect photolysis mediated by ROS and AOPs, rather than direct absorption of sunlight. Because Clindamycin has a weak absorption profile in the solar spectrum, its natural breakdown in water or soil depends on environmental sensitizers like dissolved organic matter or engineered photocatalysts. Generation of ROS are when light interacts with natural photosensitizers or semiconducting catalysts, it generates highly active chemical species. OH● radicals are the primary oxidative engine that non-selectively attacks Clindamycin molecules. Singlet oxygen (1O2) is a selective oxidizer that targetedly attacks electron-dense sites within the antibiotic structure. The attack of ROS on the clindamycin structure occurs at specific functional groups, leading to several key transformation steps. S-Oxidation is the sulfur atom in the methylthiol group of Clindamycin is highly vulnerable to singlet oxygen and OH● radical attack. This forms clindamycin sulfoxide (CSO) as a prominent primary degradation product. N-Demethylation is radical attacks on the pyrrolidine ring result in the loss of the methyl group attached to the nitrogen atom, forming N-demethyl clindamycin (NDC). Hydroxylation is OH● radicals attack the alkyl chains or the sugar backbone of the molecule, adding -OH groups to create hydroxy clindamycin sulfoxide (HCSO). Cleavage of the amide bond is sustained radical attack breaks the amide linkage that holds the lincosamide sugar portion and the amino acid portion together, splitting the antibiotic into smaller, non-toxic fragments. Kinetic studies showed that the overall photodegradation process strictly follows second-first-order kinetics, meaning the breakdown rate is proportional to the concentration of the antibiotics under optimized light intensity.

The generation of holes in the valence band occurs during the standard degradation process, which is initiated by sunlight exposure, causing electrons to move from the valence band to the conduction band. This photogenerated electron-hole pair is formed with the assistance of the GO-CuO photocatalyst. The electrons and holes can either interact with surrounding molecules or recombine. Specifically, OH● radicals are produced when water reacts with the photogenerated species on the extensive surface of the GO-CuO photocatalyst. These OH● radicals then interact with adsorbed oxygen, leading to the formation of O2- ● radicals anions. These anions are strong oxidizing agents that effectively break down the antibiotic molecules into oxidized products. The overall photodegradation mechanisms of Vancomycin, Doxycycline and Clindamycin antibiotics was illustrated (Figure 17).

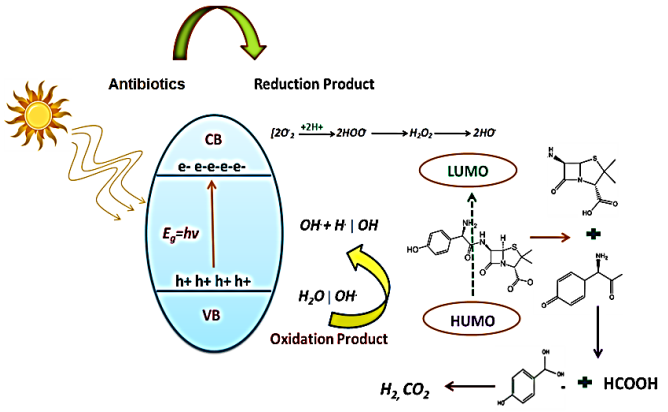

Figure 17. Degradation mechanism of Vancomycin, Doxycycline and Clindamycin antibiotics

This process highlights the critical role of the GO-CuO photocatalyst in facilitating reactive species and oxidation reactions, which are key to the effective degradation of antibiotics. Additionally, the generation of OH● radicals and superoxide anions significantly enhances the catalyst's efficiency in the antibiotic removal from wastewater system.

Reusability of GO-CuO photocatalyst

Over time, heterogeneous catalysts have been very effective and are usually preferred over homogeneous catalysts. Due to the recycling process, the heterogeneous catalyst can be used for several times without being degraded. The heterogeneous catalysts are very effective in the degradation of antibiotics. In this sudy, the as-prepared photocatalyst GO-CuO nanocomposite was reused six times to check its efficacy in the degradation of Vancomycin, Doxycycline and Clindamycin antibiotics (Figure 18).

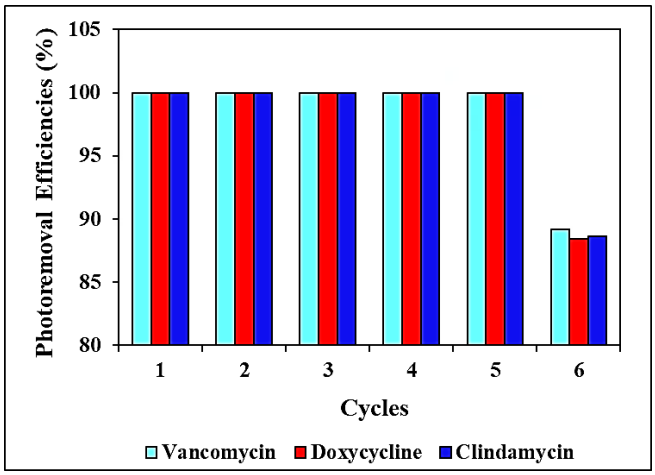

Figure 18. Reusability of GO-CuO photocatalyst under photodegradation of Vancomycin, Doxycycline and Clindamycin antibiotics.

After the 6th cycle, the degradation performance of GO-CuO nanocomposite for Vancomycin, Doxycycline and Clindamycin antibiotics were observed as 88.40-89.21%, which is good for a heterogeneous catalyst. This recycling study clearly shows that the GO-CuO nanocomposite photocatalyst is very effective even after the 6th cycle.

Conclusion

In this study, a highly active GO-CuO photocatalyst was synthesized and characterized using various techniques, including XRD, SEM, EDX, and AFM. The crystalline structure, particle size, morphology, and surface texture of the photocatalyst were thoroughly examined. The synthesized GO-CuO photocatalyst was then successfully utilized for the photodegradation of Vancomycin, Doxycycline and Clindamycin antibiotics.

After that, several parameters were fine-tuned, including a catalyst dose , a sunlight exposure, and varying volumes of NaBH4 as a proton source to achieve maximal photo degradation of Vancomycin, Doxycycline and Clindamycin antibiotics. Following optimization, the 1 mg/l GO-CuO nanocomposite demonstrated an impressive 98.70-99.00% degradation of Vancomycin, Doxycycline and Clindamycin antibiotics, respectively. The results of this study indicate that the prepared catalyst is a promising candidate for large-scale degradation of multiple antibiotics, offering a valuable tool for addressing the growing concern of antibiotic pollution in the environment.

Moreover, despite the successful photocatalytic degradation of the aforementioned antibiotics using GO-decorated copper oxide nanocomposites, certain aspects remain unexplored. Detailed mechanistic studies, including reactive species trapping experiments and advanced characterization techniques such as BET, PL, and EIS, could further elucidate charge transfer dynamics and surface properties. Additionally, the mineralization efficiency and toxicity assessment of degradation byproducts need further investigation for real-world applications. Future studies should focus on optimizing the catalyst for large-scale wastewater treatment, evaluating its stability over multiple cycles, and exploring its performance under diverse environmental conditions. Furthermore, integrating this photocatalytic system with hybrid treatment technologies could enhance its efficiency and practicality for sustainable water purification.

Acknowledgements

Experimental analyzes in this study were performed at the Laboratories of the Canada Research Center, Ottawa, Canada. The authors would like to thank this body for providing financial support.

References

1. Liu, Jian, Guizhen Yan, Zihui Huo, Yucong Mo, Yuting Wen, Weizhen Liu, Hongyu Zhou, Bing Yan, and Zhang Lin. “Thallium’s threat to aquatic life: stage-specific toxicity in zebrafish embryos and larvae.” Environment & Health 2, no. 3 (2024): 114-125.

   Crossref Google Scholar Pubmed

2. Benamar, Ahmed, Yue Tian, Florence Portet-Koltalo, M. T. Ammami, N. Giusti-Petrucciani, Yue Song, and C. Boulangé-Lecomte. “Enhanced electrokinetic remediation of multi-contaminated dredged sediments and induced effect on their toxicity.” Chemosphere 228 (2019): 744-755.

   Crossref Google Scholar Pubmed

3. Karaca, Oznur, Claudio Cameselle, and Mustafa Bozcu. “Opportunities of electrokinetics for the remediation of mining sites in Biga peninsula, Turkey.” Chemosphere 227 (2019): 606-613.

   Crossref Google Scholar Pubmed

4. Li, Shijie, Chunchun Wang, Kexin Dong, Peng Zhang, Xiaobo Chen, and Xin Li. “MIL-101 (Fe)/BiOBr S-scheme photocatalyst for promoting photocatalytic abatement of Cr (VI) and enrofloxacin antibiotic: Performance and mechanism.” Chinese Journal of Catalysis 51 (2023): 101-112.

   Crossref Google Scholar

5. Dehghani, Mohammad Hadi, Nadeem Hussain Solangi, Nabisab Mujawar Mubarak, Natarajan Rajamohan, Subrajit Bosu, Amina Othmani, Md Ahmaruzzaman et al. “MXene-based materials as adsorbents, photocatalysts, membranes and sensors for detection and removal of emerging and gaseous pollutants: A comprehensive review.” Arabian Journal of Chemistry 18, no. 1 (2025): 106052.

   Google Scholar

6. Kay, Paul, Stephen R. Hughes, James R. Ault, Alison E. Ashcroft, and Lee E. Brown. “Widespread, routine occurrence of pharmaceuticals in sewage effluent, combined sewer overflows and receiving waters.” Environmental Pollution 220 (2017): 1447-1455.

   Crossref Google Scholar Pubmed

7. Yang, Jun, and Khalid Hussain Theboc. “MXene-based Nanocomposites: An Emerging Aspirant for Removal of Antibiotics, Dyes, and Heavy Metal Ions.” Materials Chemistry Frontiers 7 (2023).

   Crossref Google Scholar

8. Hyder, Ali, Safia Sanam Memon, Shahabuddin Memon, Zafar-ul-Abdin Memon, Dhani Bux Rajpar, Samiha Gul Shaikh, and Jamil Ahmed Buledi. “A highly discerning p-tetranitrocalix [4] arene (p-TNC4) functionalized copper nanoparticles: a smart electrochemical sensor for the selective determination of diphenhydramine drug.” Microchemical Journal 163 (2021): 105908.

   Crossref Google Scholar

9. Hyder, Ali, Safia Sanam Memon, Jamil A. Buledi, Shahabuddin Memon, Zafar-ul-Abdin Memon, Samiha Gul Shaikh, and Dhani Bux Rajpar. “Strategic fabrication of para diethylamine calix [4] arene-functionalized CuO nanostructures: a metal–organic framework-based sensor for quantification of antipyrine.” Chemical Papers 77, no. 12 (2023): 7737-7748.

   Crossref Google Scholar

10. Wang, Ruming, Zhuoqin Wang, Haiping Yuan, Chunxing Li, and Nanwen Zhu. “Mechanistic exploration of COVID-19 antiviral drug ritonavir on anaerobic digestion through experimental validation coupled with metagenomics analysis.” Journal of Hazardous Materials 479 (2024): 135603.

    Crossref Google Scholar Pubmed

11. Fatta-Kassinos, Despo, Sureyya Meric, and Anastasia Nikolaou. “Pharmaceutical residues in environmental waters and wastewater: current state of knowledge and future research.” Analytical and bioanalytical chemistry 399, no. 1 (2011): 251-275.

    Crossref Google Scholar Pubmed

12. Lester, Yaal, Hadas Mamane, Ines Zucker, and Dror Avisar. “Treating wastewater from a pharmaceutical formulation facility by biological process and ozone.” Water Research 47, no. 13 (2013): 4349-4356.

    Crossref Google Scholar Pubmed

13. Tran, Ngoc Han, Martin Reinhard, and Karina Yew-Hoong Gin. “Occurrence and fate of emerging contaminants in municipal wastewater treatment plants from different geographical regions-a review.” Water research 133 (2018): 182-207.

    Crossref Google Scholar Pubmed

14. Hyder, Ali, Safia Sanam Memon, Jamil Ahmed Buledi, Shahabuddin Memon, Zafar-ul-Abdin Memon, Dhani Bux Rajpar, and Sirajuddin. “A highly selective sensor based on p-tetranitrocalix [4] arene-capped copper nanoparticles for colorimetric and bare-eye detection of cyclophosphamide.” Analytical Sciences 39, no. 12 (2023): 1981-1992.

    Crossref Google Scholar

15. Zhang, Junlei, Guojia Yu, Chaoyang Yang, and Shijie Li. “Recent progress on S-scheme heterojunction strategy enabling polymer carbon nitrides C3N4 and C3N5 enhanced photocatalysis in energy conversion and environmental remediation.” Current Opinion in Chemical Engineering 45 (2024): 101040.

    Crossref Google Scholar

16. Bielen, Ana, Ana Šimatović, Josipa Kosić-Vukšić, Ivan Senta, Marijan Ahel, Sanja Babić, Tamara Jurina, Juan José González Plaza, Milena Milaković, and Nikolina Udiković-Kolić. “Negative environmental impacts of antibiotic-contaminated effluents from pharmaceutical industries.” Water research 126 (2017): 79-87.

    Crossref Google Scholar Pubmed

17. Meng, Lingwei, Xiangkun Li, Xinran Wang, Kaili Ma, Gaige Liu, and Jie Zhang. “Amoxicillin effects on functional microbial community and spread of antibiotic resistance genes in amoxicillin manufacture wastewater treatment system.” Journal of Environmental Sciences 61 (2017): 110-117.

Crossref Google Scholar Pubmed

18. Chen, Baowei, Lan Lin, Ling Fang, Ying Yang, Enzhong Chen, Ke Yuan, Shichun Zou, Xiaowei Wang, and Tiangang Luan. “Complex pollution of antibiotic resistance genes due to beta-lactam and aminoglycoside use in aquaculture farming.” Water research 134 (2018): 200-208.

Crossref Google Scholar Pubmed

19. Dutta, Suvanka, Ananya Ghosh, Sankar Chandra Moi, and Rajnarayan Saha. “Application of response surface methodology for optimization of reactive azo dye degradation process by Fenton’s oxidation.” International Journal of Environmental Science and Development 6, no. 11 (2015): 818-823.

Google Scholar

20. Sharma, Ashish, Manisha Verma, and A. K. Haritash. “Degradation of toxic azo dye (AO7) using Fenton’s process.” Advances in environmental research 5, no. 3 (2016): 189-200.

Google Scholar

21. Monteoliva-García, A., J. Martín-Pascual, M. M. Muñío, and J. M. Poyatos. “Removal of carbamazepine, ciprofloxacin and ibuprofen in real urban waste water by using light-driven advanced oxidation processes.” International journal of environmental science and technology 16, no. 10 (2019): 6005-6018.

Crossref Google Scholar

22. Hyder, Ali, Muzamil Thebo, Dahar Janwery, Jamil Ahmed Buledi, Imamdin Chandio, Awais Khalid, Bader S. Al-Anzi et al. “Fabrication of para-dimethylamine calix [4] arene functionalized self-assembled graphene oxide composite material for effective removal of 2, 4, 6-tri-Cholorphenol from aqueous environment.” Heliyon 9, no. 9 (2023).

Crossref Google Scholar Pubmed

23. Khilji, Meher-Un-Nisa, Aijaz Ali Otho, Roomia Memon, Awais Khalid, Mohsin Kazi, Ali Hyder, Dahar Janwery et al. “Facile fabrication of a free-standing magnesium oxide-graphene oxide functionalized membrane: a robust and efficient material for the removal of pollutants from aqueous matrices.” Analytical Letters 57, no. 13 (2024): 2067-2084.

Crossref Google Scholar

24. Rajpar, Dhani Bux, Ali Hyder, Abdul Wahab Memon, Fakhar N. Memon, Shahabuddin Memon, Azhar Uddin, Ayaz Ali Memon, Mohsin Kazi, and Khalid Hussain Thebo. “Versatility of p-Imidazolemethylcalix [4] arene-attached silica resin for the removal of lead and cadmium ions from wastewater.” International Journal of Environmental Analytical Chemistry 105, no. 13 (2025): 2941-2956.

Crossref Google Scholar

25. Xu, Bincheng, Ze Lin, Fengting Li, Tao Tao, Gong Zhang, and Ying Wang. “Local O2 concentrating boosts the electro-Fenton process for energy-efficient water remediation.” Proceedings of the National Academy of Sciences 121, no. 11 (2024): e2317702121.

Crossref Google Scholar

26. Choi, Jonghoon, Hana Oh, Sang-Wook Han, Seokhoon Ahn, Jaegeun Noh, and Joon B. Park. “Preparation and characterization of graphene oxide supported Cu, Cu2O, and CuO nanocomposites and their high photocatalytic activity for organic dye molecule.” Current Applied Physics 17, no. 2 (2017): 137-145.

Crossref Google Scholar

27. Anjum, Farhana, Abdullah M. Asiri, Murad Ali Khan, M. I. Khan, Sher Bahadar Khan, Kalsoom Akhtar, Esraa M. Bakhsh, Khalid A. Alamry, Soliman Yahya Alfifi, and Sudip Chakraborty. “Photo-degradation, thermodynamic and kinetic study of carcinogenic dyes via zinc oxide/graphene oxide nanocomposites.” Journal of Materials Research and Technology 15 (2021): 3171-3191.

Crossref Google Scholar

28. Nahyoon, Noor Ahmed, Mujahid Mehdi, Khalid Hussain Thebo, Nasrullah Mahar, Ayaz Ali Memon, Najma Memon, and Nadir Hussain. “Synthesis of novel visible light driven MgO@ GO nanocomposite photocatalyst for degradation of Rhodamine 6G.” Optical Materials 135 (2023): 113260.

Crossref Google Scholar

29. Soomro, Faheeda, Fida Hussain Memon, Muhammad Ali Khan, Muzaffar Iqbal, Aliya Ibrar, Ayaz Ali Memon, Jong Hwan Lim, Kyung Hyon Choi, and Khalid Hussain Thebo. “Ultrathin graphene oxide-based nanocomposite membranes for water purification.” Membranes 13, no. 1 (2023): 64.

Crossref Google Scholar Pubmed

30. Wu, Cheng-Hung, Chueh-Han Wang, Ming-Tsung Lee, and Jeng-Kuei Chang. “Unique Pd/graphene nanocomposites constructed using supercritical fluid for superior electrochemical sensing performance.” Journal of Materials Chemistry 22, no. 40 (2012): 21466-21471.

Crossref Google Scholar

31. Habte, Adere Tarekegne, and Delele Worku Ayele. “Synthesis and characterization of reduced graphene oxide (rGO) started from graphene oxide (GO) using the tour method with different parameters.” Advances in Materials Science and Engineering 2019, no. 1 (2019): 5058163.

Crossref Google Scholar

32. Buledi, Jamil A., Amber R. Solangi, Arfana Mallah, Zia-ul-Hassan Shah, Syed Tufail Sherazi, Muhammad Raza Shah, Ali Hyder, and Saba Ali. “Electrochemical monitoring of isoproturon herbicide using NiO/V2O5/rGO/GCE.” Journal of Food Measurement and Characterization 17, no. 2 (2023): 1628-1639.

Crossref Google Scholar

33. Hyder, Ali, Akbar Ali, Awais Khalid, Ahmed Nadeem, Muhammad Ali Khan, Abdul Wahab Memon, Ayaz Ali Memon et al. “Supramolecular structural-based graphene oxide lamellar membrane for removing environmental pollutants from wastewater.” Industrial & Engineering Chemistry Research 62, no. 49 (2023): 21335-21346.

Google Scholar

34. Kositzi, M., A. Antoniadis, I. Poulios, I. Kiridis, and S. Malato. “Solar photocatalytic treatment of simulated dyestuff effluents.” Solar Energy 77, no. 5 (2004): 591-600.

Crossref Google Scholar

35. Buledi, Jamil A., Abdul H. Pato, Ali H. Kanhar, Amber R. Solangi, Madeeha Batool, Sidra Ameen, and Ismail M. Palabiyik. “Heterogeneous kinetics of CuO nanoflakes in simultaneous decolorization of Eosin Y and Rhodamine B in aqueous media.” Applied Nanoscience 11, no. 4 (2021): 1241-1256.

Crossref Google Scholar

36. Bhutto, Toqeer Ahmed, Mushtaque Ali Jakhrani, Ahmed Ali Jamali, Jamil A. Buledi, Raja Dahar Janwary, Ali Hyder, Khalid Hussain Chachar, and Nazar Hussain Kalwar. “Strategic fabrication of PVP caped CuO hetero-catalyst for degradation of Eosin Y: a decontamination study.” Journal of the Iranian Chemical Society 20, no. 5 (2023): 1225-1235.

Crossref Google Scholar

37. Li, Shijie, Ruyu Yan, Mingjie Cai, Wei Jiang, Mingyi Zhang, and Xin Li. “Enhanced antibiotic degradation performance of Cd0.5Zn0.5S/Bi2MoO6 S-scheme photocatalyst by carbon dot modification.” Journal of Materials Science & Technology 164 (2023): 59-67.

Crossref Google Scholar

38. Janani, B., V. Vinotha Sre, Asad Syed, Abdallah M. Elgorban, Islem Abid, Ling Shing Wong, and S. Sudheer Khan. “Engineering the S-scheme heterojunction between NiFeAl-LDH and BiOCOOH nanoflower by constructing an interfacial electric field for efficient degradation of levofloxacin under visible light.” Journal of Water Process Engineering 66 (2024): 105986.

Crossref Google Scholar

39. Li, Shijie, Ke Rong, Xiaoqin Wang, Chuqi Shen, Fang Yang, and Qinghong Zhang. “Design of carbon quantum dots/CdS/Ta3N5 S-scheme heterojunction nanofibers for efficient photocatalytic antibiotic removal.” Acta Physico-Chimica Sinica 40, no. 12 (2024): 2403005.

Crossref Google Scholar

40. Sre, V. Vinotha, Mohammad K. Okla, B. Janani, Mostafa A. Abdel-Maksoud, Saud S. Al-Amri, Ibrahim A. Alaraidh, Abdulrahman A. Alatar, and S. Sudheer Khan. “A novel sunlight driven Z scheme ZnCdS QDs deposited over g-C3N4 photocatalyst for photoinactivation of E. coli cells.” Journal of Water Process Engineering 59 (2024): 104957.

Crossref Google Scholar

41. Sre, V. Vinotha, B. Janani, Asad Syed, Abdallah M. Elgorban, Islem Abid, Ling Shing Wong, and S. Sudheer Khan. “Unveiling the enhanced photocatalytic degradation of metronidazole over green-synthesized Ag@ ZnCdS QDs Schottky heterojunction: Pathway, toxicity evaluation and mechanistic insights.” Journal of Water Process Engineering 62 (2024): 105325.

Crossref Google Scholar

42. Zhuang, Qian, Xueping Li, Xiaoyan Lian, Huanting Hu, Nan Wang, Jiawei Wu, Kangkang Miao, Guodong Feng, and Xiaolin Luo. “Catalysis enhancement of Co_3O_4 through the epitaxial growth of inert ZnO in peroxymonosulfate activation: the catalytic mechanism of surface hydroxyls in singlet oxygen generation.” Crystal Growth & Design 25, no. 2 (2024): 319-329.

Crossref Google Scholar

43. Khan, S. Sudheer, J. P. Steffy, S. Swetha, Asad Syed, Abdallah M. Elgorban, Alanoud T. Alfagham, Meenakshi Verma, and Ling Shing Wong. “Sulfur vacancies engineered self-supported CdCr2S4 as cascade nanoreactor for efficient photocatalytic degradation of rifampicin.” Journal of Water Process Engineering 69 (2025): 106619.

Crossref Google Scholar

44. Ali, Zareen Suhara Nazeer, Mohammad K. Okla, S. Kokilavani, Mostafa A. Abdel-Maksoud, Abdulrahman A. Alatar, P. R. Sivaranjani, Saud S. Al-Amri, Ibrahim A. Alaraidh, and S. Sudheer Khan. “Unravelling the enhanced rifampicin photocatalytic degradation over green-synthesized SrO2@ SnIn4S8 pn heterojunction: Pathway, toxicity evaluation and mechanistic insights.” Chemosphere 352 (2024): 141464.

Crossref Google Scholar Pubmed

45. Brindha, B., Mohammad K. Okla, S. Kokilavani, L. Sabariselvan, Saud S. Al-amri, Mostafa A. Abdel-Maksoud, G. Harini, Raida Alshuwaish, Waleed A. Alsakkaf, and S. Sudheer Khan. “Dynamic Ag-mediated electron transfer confined ZnO nanorods for boosted photocatalytic bacterial disinfection.” Journal of Cleaner Production 451 (2024): 141908.

Crossref Google Scholar

46. Sruthi, L., Mohammad K. Okla, B. Janani, Mostafa A. Abdel-Maksoud, Ibrahim A. Saleh, Hashem A. Abu-Harirah, and S. Sudheer Khan. “Construction of rGO-Bi2Sn2O7-NiFe2O4 nanoheterojunction system for the enhanced photodegradation of doxycycline: A brief insight on degradation kinetics and toxicological evaluation on Allium cepa.” Journal of Cleaner Production 434 (2024): 139936.

Crossref Google Scholar

47. Fan, Weitao, Qi Xin, Yuanhang Dai, Yijie Chen, Shaojun Liu, Xiao Zhang, Yang Yang, and Xiang Gao. “Competitive transport and adsorption of CO2/H2O in the graphene nano-slit pore: A molecular dynamics simulation study.” Separation and Purification Technology 353 (2025): 128394.

Crossref Google Scholar

48. Sabariselvan, L., Asad Syed, J. P. Steffy, Abdallah M. Elgorban, Islem Abid, Ling Shing Wong, and S. Sudheer Khan. “Engineering sulfur defect rich Vs-ZnS with sulfur vacancies modulated charge transfer for high performance photocatalytic degradation of levofloxacin.” Journal of Water Process Engineering 69 (2025): 106761.

Crossref Google Scholar

49. Steffy, J. P., Alanoud T. Alfagham, Abdallah M. Elgorban, and S. Sudheer Khan. “Morphology transition engineering of WO3 from 1D nanorods to single-crystalline 3D nanocubes grafted with 2D g-C3N4 decorated with 0D SnS2 QDs for pharmaceutical waste photodegradation.” Journal of Water Process Engineering 69 (2025): 106728.

Crossref Google Scholar

50. Steffy, J. P., Asad Syed, Chinnaperumal Kamaraj, Selvam Naveenkumar, Ajith M. Thomas, Abdallah M. Elgorban, Islem Abid, Lija L. Raju, Ling Shing Wong, and S. Sudheer Khan. “Facet engineering in Au nanoparticles buried in Cu2O nanocubes for enhanced catalytic degradation of rhodamine B and larvicidal application.” Sustainable Materials and Technologies 43 (2025): e01185.

Crossref Google Scholar

51. Dong, Lifeng, Raghavendar Reddy Sanganna Gari, Zhou Li, Michael M. Craig, and Shifeng Hou. “Graphene-supported platinum and platinum–ruthenium nanoparticles with high electrocatalytic activity for methanol and ethanol oxidation.” Carbon 48, no. 3 (2010): 781-787.

Crossref Google Scholar

52. An, Xiaoqiang, Jimmy C. Yu, Yu Wang, Yongming Hu, Xuelian Yu, and Guangjin Zhang. “WO3 nanorods/graphene nanocomposites for high-efficiency visible-light-driven photocatalysis and NO2 gas sensing.” Journal of Materials Chemistry 22, no. 17 (2012): 8525-8531.

Crossref Google Scholar

53. Low, Jingxiang, Jiaguo Yu, and Wingkei Ho. “Graphene-based photocatalysts for CO2 reduction to solar fuel.” The journal of physical chemistry letters 6, no. 21 (2015): 4244-4251.

Crossref Google Scholar Pubmed

54. Rehman, Faisal, Fida Hussain Memon, Akbar Ali, Shah Masaud Khan, Faheeda Soomro, Muzaffar Iqbal, and Khalid Hussain Thebo. “Recent progress on fabrication methods of graphene-based membranes for water purification, gas separation, and energy sustainability.” Reviews in Inorganic Chemistry 43, no. 1 (2023): 13-31.

Crossref Google Scholar

55. Sun, Hongmei, Linyuan Cao, and Lehui Lu. “Magnetite/reduced graphene oxide nanocomposites: one step solvothermal synthesis and use as a novel platform for removal of dye pollutants.” Nano Research 4, no. 6 (2011): 550-562.

Crossref Google Scholar

56. Shan, Zezhi, Yanrong Yang, Haoran Shi, Jiali Zhu, Xiao Tan, Yi Luan, Zhenqi Jiang, Ping Wang, and Jieling Qin. “Hollow dodecahedra graphene oxide-cuprous oxide nanocomposites with effective photocatalytic and bactericidal activity.” Frontiers in Chemistry 9 (2021): 755836.

Crossref Google Scholar Pubmed

57. Sharif, Shania, Khuram Shahzad Ahmad, Fida Hussain Memon, Faisal Rehman, Faheeda Soomro, and Khalid Hussain Thebo. “Functionalised graphene oxide-based nanofiltration membranes with enhanced molecular separation performance.” Materials Research Innovations 26, no. 6 (2022): 373-381.

Crossref Google Scholar

58. Hyder, Ali, Jamil Ahmed Buledi, Roomia Memon, Anjum Qureshi, Javed H. Niazi, Amber Rehana Solangi, Shahabuddin Memon, Ayaz Ali Memon, and Khalid Hussain Thebo. “Modified electrochemical sensor via supramolecular structural functionalized graphene oxide for ultra-sensitive detection of gallic acid.” Diamond and Related Materials 139 (2023): 110357.

Crossref Google Scholar

59. de Jesus, Roberta A., Geovânia C. de Assis, Rodrigo José de Oliveira, José Arnaldo S. Costa, Caio Marcio P. da Silva, Hafiz MN Iqbal, and Luiz Fernando R. Ferreira. “Metal/metal oxide nanoparticles: A revolution in the biosynthesis and medical applications.” Nano-Structures & Nano-Objects 37 (2024): 101071.

Crossref Google Scholar

60. Truong, Thi Thuy, Sudip Mondal, Vu Hoang Minh Doan, Soonhyuk Tak, Jaeyeop Choi, Hanmin Oh, Tan Dung Nguyen, Mrinmoy Misra, Byeongil Lee, and Junghwan Oh. “Precision-engineered metal and metal-oxide nanoparticles for biomedical imaging and healthcare applications.” Advances in colloid and interface science 332 (2024): 103263.

Crossref Google Scholar

61. Rajput, V. D., T. Minkina, S. Suskova, S. Mandzhieva, V. Tsitsuashvili, V. Chapligin, and A. Fedorenko. “Effects of copper nanoparticles (CuO NPs) on crop plants: a mini review.” BioNanoScience 8, no. 1 (2018): 36-42.

Crossref Google Scholar

62. Hou, Jing, Xiangxue Wang, Tasawar Hayat, and Xiangke Wang. “Ecotoxicological effects and mechanism of CuO nanoparticles to individual organisms.” Environmental pollution 221 (2017): 209-217.

Crossref Google Scholar Pubmed

63. Hoffmann, Michael R., Scot T. Martin, Wonyong Choi, and Detlef W. Bahnemann. “Environmental applications of semiconductor photocatalysis.” Chemical reviews 95, no. 1 (1995): 69-96.

Crossref Google Scholar

64. Kutsuna, Shuzo, Yumiko Nagaoka, Koji Takeuchi, and Hisao Hori. “TiO2-induced heterogeneous photodegradation of a fluorotelomer alcohol in air.” Environmental science & technology 40, no. 21 (2006): 6824-6829.

Crossref Google Scholar Pubmed

65. 65. Panchangam, Sri Chandana, Angela Yu-Chen Lin, Khaja Lateef Shaik, and Cheng-Fang Lin. “Decomposition of perfluorocarboxylic acids (PFCAs) by heterogeneous photocatalysis in acidic aqueous medium.” Chemosphere 77, no. 2 (2009): 242-248.

Crossref Google Scholar Pubmed

66. Qu, Yan, Chaojie Zhang, Fei Li, Jing Chen, and Qi Zhou. “Photo-reductive defluorination of perfluorooctanoic acid in water.” Water research 44, no. 9 (2010): 2939-2947.

Crossref Google Scholar Pubmed

67. Holst, Amanda J., Soma Bahmany, Angela CJ van Dorp, Jakob van Oldenrijk, P. Koen Bos, Ewout S. Veltman, Brenda CM de Winter, and Birgit CP Koch. “Quantification of Vancomycin and Clindamycin in Synovial Tissue and Bone Using Ultra-High-Performance Liquid Chromatography-Tandem Mass Spectrometry.” Therapeutic Drug Monitoring (2022): 10-1097.

Crossref Google Scholar Pubmed

68. Farzadkia, Mahdi, Kourosh Rahmani, Mitra Gholami, Ali Esrafili, Ayat Rahmani, and Hassan Rahmani. “Investigation of photocatalytic degradation of clindamycin antibiotic by using nano-ZnO catalysts.” Korean Journal of Chemical Engineering 31, no. 11 (2014): 2014-2019.

Crossref Google Scholar

69. Tong, Yanbin, Jing Kang, Jimin Shen, Zhonglin Chen, Shengxin Zhao, Liqun Sun, and Weiqiang Wang. “Effective degradation of doxycycline by photocatalytic BiVO4–H2O2 under visible light.” Environmental Progress & Sustainable Energy 38, no. 6 (2019): e13259.

Crossref Google Scholar

70. Dehghani, Fatemeh, Saeed Yousefinejad, Mansooreh Dehghani, Seyed Mehdi Borghei, and Amir Hossein Javid. “Vancomycin removal using TiO2–clinoptilolite/UV in aqueous media and optimisation using response surface methodology.” International Journal of Environmental Analytical Chemistry 104, no. 16 (2024): 4451-4469.

Crossref Google Scholar

71. Verma, Panchraj, Subrata Das, Shubham Raj, and Raphaël Schneider. “A Rapid and Complete Photodegradation of Doxycycline Using rGO@ CuO Nanocomposite Under Visible and Direct Sunlight: Mechanistic Insights and Real-Time Applicability.” Nanomaterials 15, no. 13 (2025): 953.

Crossref Google Scholar Pubmed

Citation: Delia, Teresa S, Öztekin R. “Photoremovals of Vancomycin, Doxycycline and Clindamycin Antibiotics via Graphene Oxide Decorated with Copper Oxide (GO-CuO) Nanocomposites under Sun Light”. J Pharmacol Drug Deliv (2026): 108. DOI: 10.59462/JPDD.4.1.108.